8-2003

Probabilistic Based Design of FRP Structures

Maha Khader Alqam
University of Tennessee - Knoxville

To the Graduate Council:

I am submitting herewith a dissertation written by Maha Khader Alqam entitled "Probabilistic Based Design of FRP Structures." I have examined the final electronic copy of this dissertation for form and content and recommend that it be accepted in partial fulfillment of the requirements for the degree of Doctor of Philosophy, with a major in Civil Engineering.

Richard Bennett, Major Professor

We have read this dissertation and recommend its acceptance:

Edwin Burdette, Eric Drumm, Chris Pionke

Accepted for the Council:
Dixie L. Thompson

Vice Provost and Dean of the Graduate School

(Original signatures are on file with official student records.)

To the Graduate Council:

I am submitting herewith a dissertation written by Maha Khader Alqam entitled "Probabilistic Based Design of FRP Structures." I have examined the final electronic copy of this dissertation for form and content and recommended that it be accepted in partial fulfillment of the requirements for the degree of Doctor of Philosophy, with a major in Civil Engineering.

Richard Bennett
Major Professor

We have read this dissertation
and recommend its acceptance:

Edwin Burdette

Eric Drumm

Chris Pionke

Acceptance for the Council:

Anne Mayhew
Vice Provost and
Dean of Graduate Studies

(Original signatures are on file with official student records)

PROBABILISTIC BASED DESIGN OF FRP STRUCTURES

A Dissertation
Presented for the
Doctor of Philosophy
Degree
The University of Tennessee, Knoxville

Maha Khader Alqam
August 2003

ACKNOWLEDGEMENTS

I would like to express my gratitude and appreciation to my major professor Dr. Richard Bennett for his guidance and support he provided during my pursuit of the Doctoral Degree. I would like also to acknowledge the helpful comments and suggestions provided by the members of my committee, Dr. Edwin Burdette, Dr. Eric Drumm, and Dr. Chris Pionke. Finally, I would like to thank my parents for their endless support during my studies at The University of Tennessee.

ABSTRACT

This thesis presents the results of an analytical probabilistic based design procedure for concentrically loaded compression members and simply supported beams of fiber-reinforced polymeric (FRP) composite materials. Resistance factors for use in an LRFD format are developed for columns for both flexural buckling and local buckling of doubly symmetric sections, both flexural buckling and flexural-torsional buckling of equal leg angles, and material failure. Resistance factors are developed for lateral-torsional buckling of simply supported doubly symmetric beams loaded with concentrated vertical loads at mid-spans. The developed resistance factors are a function of the coefficient of variation of the appropriate material properties. The proposed resistance factors were determined to provide a reliability index of 3.0 for stability failure modes and a reliability index of 3.5 for the material failure mode.

TABLE OF CONTENTS

LIST OF TABLES

LIST OF FIGURES

CHAPTER 1

INTRODUCTION

A composite material system is a combination of two or more materials in order to produce better specific mechanical performance and physical properties than any single material on its own. One type of composite material that is gaining use in structural engineering applications is fiber-reinforced polymer (FRP) composites.

The most important component of fiber reinforced polymer (FRP) composite structural elements is the fiber (the reinforcement of a composite system). It is used to provide adequate strength and stiffness. Typically, pultruded composites have 40-80 percent fibers by volume. Glass fibers (E-Glass, Z-Glass and S-Glass) and carbon fibers are the major fibers used for civil composites. The other component of the FRP composite is the polymer resin matrix that binds the fibers together, transfers the loads into fibers, and protects the fibers against environmental damages. Polyesters, vinylesters, and epoxy resins are the most popular resins used for civil structural applications.

The most popular techniques for manufacturing structural FRP composite are pultrusion and hand lay-up techniques. The pultrusion manufacturing is a fully automated controlled process. It is used to produce straight, long members, as well as open and solid geometrical shaped (I-shapes, box, wide flange, and tube sections) members. A machine called “the puller” is used in this process to pull the raw materials. It consists of pulling pads that grip the product and a drive system that keeps the product moving. This machine is located just before the

final cut-off saw. Typically, the process starts with the unidirectional glass roving (fiber runs along the length of the profile). Then the fiberglass mat (a multidirectional reinforcement) is added in. Finally, the glass is wetted out with the liquid resin and pulled into a heated die where the product changes from liquid to a solid profile. After the profile exits the die, it gets pulled by the puller and cut to the desired length.

The hand lay-up technique is the oldest and simplest. It is used for manufacturing both small and large reinforced products. Multi-directional fiber reinforcement can be used. The reinforcing mat is positioned in the open mold; then the resin is poured, brushed or sprayed over and into the glass. This technique is used for the cases where fibers with different orientations are required.

Fiber reinforced polymer (FRP) composite structural elements have a high strength-to-weight ratio. They are corrosion-resistant, do not decay deteriorate, and are nonconductive. Generally, they have good fatigue properties and are resistant to freeze-thaw damage. On the other hand, FRP elements have features that are problematic in structural design, such as their lack of ductility and low stiffness. The modulus of elasticity is 25% of the modulus of elasticity of steel. Thus, limit states which are a function of stiffness, such as buckling and serviceability issues, are relatively more important for design considerations. Because of the high strength/stiffness ratio of the FRP composites, the design of most FRP structures is controlled by deformation rather than by strength. Most FRP composite structural components behave linearly under load till failure,

unlike steel where the redistribution of load follows the initial yielding. FRP material costs are greater than concrete and steel materials. However, reduced weight, increased speed of construction or lower maintenance offset the higher initial cost of FRP materials.

Hindering the increased use of FRP composites is the lack of established design standards. Chambers (1997) presented a proposed draft outline of a standard which was based on load and resistance factor design (LRFD). Probabilistic based load factors have been well established (e.g. ASCE 7) but there is the need to develop both design equations and associated resistance factors for FRP members.

This dissertation presents the development of a probabilistic based code for FRP members. A target safety level is determined. Since the variability of FRP material properties is a function of fiber type, fiber volume, lay-up and quality control procedures, the resistance factors are developed as a function of the coefficient of variation (CV) of the material properties. Thus, a manufacturer would need to provide information on the CV of their product to the structural engineer. Manufacturers who provide material with a smaller CV would be rewarded by having the design code specify a larger resistance factor.

Specifically, proposed design equations and related resistance factors for concentrically loaded FRP pultruded compression members and simply supported beams with concentrated loads at mid-spans, under short-term loading are developed. Limit states considered for columns are flexural buckling and local buckling of doubly symmetric sections, both flexural buckling and flexural-

torsional buckling of equal leg angles, and material failure. Lateral-torsional buckling limit state is considered for doubly symmetric simply supported beams. The effects of long-term behavior such as creep and duration of load effects are beyond the scope of the present investigation.

CHAPTER 2

LITERATURE REVIEW

In the past several years, a number of experimental and analytical studies have been performed in order to develop design guidelines for FRP composite members.

2.1 CONCENTRIC COLUMNS (GLOBAL BUCKLING)

Zureick and Scott (1997) investigated experimentally the short-term behavior of concentrically loaded FRP composite slender members. Design guidelines and a step-by-step example were provided. A total of 24 specimens of box and I-shape cross-sections with effective slenderness ratios ranging from 36 to 103 were used in this study. The test results were compared to the following analytical formulas (Zureick and Scott, 1997):

$$P_E = \frac{\pi^2 \; E_L \; I_{\min}}{L^2} \tag{2.1}$$

$$P_e = \frac{P_E}{1 \; + \; (\frac{n_s \; P_E}{A_g \, G_{LT}})} \tag{2.2}$$

where, P_E is the buckling load as proposed by Hewson (1978) which is a modified form of the familiar Euler buckling equation, P_e is the critical buckling load of a slender composite column proposed by Engesser (1989), E_L is the elastic modulus of elasticity in the longitudinal direction, $I_{\min}$ is the moment of inertia about the minor principal axis, L is the length, G_{LT} is the in plane shear modulus of elasticity, n_s is the form factor for shear, and A_g is the gross area.

Tests were performed to estimate the longitudinal elastic properties (E_L^c , E_L^t , F_L^c and F_L^t), and in plane shear properties (G_{LT} , F_v).

where,

E_L^c : longitudinal modulus from compression tests.

E_L^t : longitudinal modulus from tension tests.

F_L^c : ultimate strength from compression tests.

F_L^t : ultimate strength from tension tests.

G_{LT} : in-plane shear modulus.

F_v : ultimate shear stress.

The percentage-difference between E_L^t and E_L^c ranged from 0.3 to 10.3. Thus, E_L^c was recommended to use as E_L in the design equations and guidelines. The experimental buckling loads were determined and compared with the predicted ones using equations 2.1 and 2.2. The ratios of the experimental buckling loads to the analytical buckling loads using equations 2.1 and 2.2 developed by Zureick and Scott (1997) were used in this investigation. Design guidelines for concentrically loaded unidirectional FRP members were recommended as follows,

$$P_r = \phi_c P_n \tag{2.3}$$

where, ϕ_c is the resistance factor and P_n is the nominal compressive resistance. They suggested a ϕ_c factor of 0.85. P_n is defined as:

$$P_n = A_g F_{cr} \tag{2.4}$$

where, A_g is the gross area of the column and F_{cr} is the critical buckling stress,

$$F_{cr} = \eta_s F_E \leq F_L^c \tag{2.5}$$

where, F_E is the elastic buckling stress, and η_s is the shear deformation parameter.

$$F_E = \frac{\pi^2 E_L}{(L_{eff} / r)^2} \tag{2.6}$$

$$\eta_s = \frac{1}{1 + [n_s \pi^2 / (L_{eff} / r)^2](E_L G_{LT})} \tag{2.7}$$

Where, L_{eff} is the effective length of the column.

Barbero and Tomblin (1993) experimentally determined the critical loads and investigated global buckling for I-shaped FRP long columns. Tests were performed on I-shaped FRP cross-sections (4 in. x 4 in. x ¼ in., 6 in. x 6 in. x ¼ in., and 6 in. x 6 in. x 3/8 in.) with lengths ranging from 4 ft. to 20 ft. The experimentally determined buckling loads were compared with the theoretically predicted loads as follows:

$$P_{cr} = \frac{\pi^2 D}{L^2} \tag{2.8}$$

where, L is the column length and D is the bending stiffness. Southwell's method was used to determine the buckling loads using a data deduction technique on the hyperbolic experimental results about the weak and strong axes (Southwell, 1932). The long column tests were performed using a Material Testing System (MTS) for weak and strong axes. For the weak axis, all buckling loads were below the theoretical prediction. Thus, the theoretical load can be considered the

upper bound for the actual buckling load because the theoretical value assumes perfect lay up and manufacturing conditions. The ratio of the experimental buckling load to the analytical buckling load ranged from 0.94 to 1.01 with an average of 0.96 and a standard deviation of 0.02. For the strong axis, the critical loads for several cross-sections were not obtained because of the machine capacity. All failure loads were below the theoretical value. Although the theoretical buckling load was always high, all percentage differences between the experimental and the theoretical loads were less than 6.2 percent. The predicted (Euler) buckling loads for long columns are very accurate even for complex materials. The results developed by Barbero and Tomblin (1993) are very close to the results developed for I-shaped FRP cross-section columns by Zureick and Scott (1997). Zureick and Scott (1997) had an average of 0.93 (< 4% difference) for the ratios of the experimental buckling loads and the analytical buckling loads using equation 2.1.

Zureick and Steffen (2000) conducted a short-term experimental behavior investigation for concentrically loaded equal-leg single angle members made of pultruded FRP material. The experiment was conducted on 25 specimens. A detailed material study was performed on all tested specimens to obtain the relevant orthotropic material constants E_T, G_{LT}, and ν_{LT} (transverse elastic modulus, in-plane shear modulus and major Poisson's ratio respectively), as well as the ultimate compressive and the in-plane shear strengths. An average value for Poisson's ratio was found to be $\nu_{LT} = 0.3$.

For loaded polymeric composite single angle members with single

symmetrical cross section about the y-axis, the buckling occurs in either a flexural mode (flexure about the minor z-axis) or a flexural-torsional mode (flexure about the major y-axis and twist about the member longitudinal x-axis).

For the flexural mode, the critical buckling load can be shown to have the form (Zureick and Steffen, 2000):

$$P_{ez} = \frac{\pi^2 E_L}{\left(\frac{K_z L_z}{r_z}\right)^2} A_g \tag{2.9}$$

where,

P_{ez} : flexural buckling load about the z-axis.

A_g : gross sectional area.

E_L :longitudinal modulus of elasticity.

K_z L_z : effective length for bending about the principal z-axis.

r_z : radius of gyration about z-axis.

Seven specimens failed in this mode. The experimental flexural buckling loads ($P_{\exp}$) were compared with those predicted theoretically (P_{pred}) using equation (2.9).

For the flexural-torsional mode, the critical buckling load can be shown to have the form (Zureick and Steffen, 2000):

$$P_{ft} = \frac{P_{ey} + P_{ex}}{2H}\left[1 - \sqrt{1 - \frac{4H\, P_{ey} P_{ex}}{(P_{ey} + P_{ex})^2}}\right] \tag{2.10}$$

in which,

$$P_{ey} = \frac{\pi^2 E_L}{\left(\frac{K_y L_y}{r_y}\right)^2} A_g \tag{2.11}$$

$$P_{ex} = \frac{1}{r_p^2}\left[\frac{\pi^2 D_w}{(K_x L_x)^2} + D_t\right] \tag{2.12}$$

where,

P_{ft} : flexural-torsional buckling load.

P_{ey} : flexural buckling load about the y-axis.

P_{ex} : torsional buckling load about the longitudinal x-axis.

K_y $\mathrm{L_y}$: effective length for bending about the principal y-axis.

K_x $\mathrm{L_x}$: effective length for twisting about the longitudinal x-axis.

r_y : radius of gyration about y-axis.

D_w , D_t : warping rigidity and torsional rigidity respectively.

r_p : combined geometrical and material constant.

For the angle problem discussed in this investigation the parameters D_w , D_t , H and r_p^2 are equal to:

$$D_w = \frac{E_L}{(1 - \nu_{LT}\nu_{TL})}\frac{A_g^3}{144}$$

$$D_t = G_{LT}\frac{2b\ t^3}{3}$$

$$H = \frac{5}{8}$$

$$r_p^2 \approx \frac{b^2}{3}$$

where,

ν_{LT} : major Poisson's ratio.

ν_{TL} : minor Poisson's ratio.

b: leg width.

t: leg thickness.

Substituting the values of the parameters into the formula for P_{ex} and rearranging, then P_{ex} can be shown to have the formula:

$$P_{ex} = \left[\frac{G_{LT}}{(b/t)^2} + \frac{\pi^2 E_L}{12(1-\nu_{LT}\nu_{TL})(K_x L_x / t)^2} \right] A_g \qquad (2.13)$$

The experimental flexural-torsional buckling loads were compared to the theoretical loads from equation 10 using $L_x = L_y = L$ and $K_x = K_y = 1.0$, even though K_y is somewhere between 0.5 for fixed and 1.0 for pinned boundaries. When E_L / G_{LT} <20, the flexural-torsional buckling load P_{ft} is 90% of the torsional buckling load P_{ex}. The computed value of the flexural-torsional buckling value will not change significantly if K_y changes from 1.0 to 0.5. To examine the influence of the effective length on torsion (K_x varies from 0.5 when the angle ends are restrained, to 1.0, when the angle ends are free to wrap), equation (2.13) was conservatively approximated in the case of an equal leg angle to the equation:

$$P_{ex} = \left[\frac{G_{LT}}{(b/t)^2} + \frac{\pi^2 E_L}{12 (K_x L_x / t)^2} \right] A_g \tag{2.14}$$

For practical angle lengths and for materials with E_L / G_{LT} values equal to or less than 5.5, the second term of (2.14) is negligible when K_x is assumed equal to 1.0. Also the flexural-torsional buckling load is approximately equal to 90% of that of torsional buckling. So, for practicality, for the case of polymeric composite equal-leg angles reinforced with fibers having a longitudinal modulus equal to or less than that of the glass, the flexural buckling load can be estimated using the following simplified equation:

$$P_{ft} \approx 0.9 P_{ex} = 0.9 \frac{G_{LT}}{\left(\frac{b}{t}\right)^2} A_g \tag{2.15}$$

Eighteen specimens failed in this mode. The experimental flexural buckling loads ($P_{\exp}$) were compared to those predicted theoretically (P_{pred}) using equations 2.13 and 2.15. The ratios of the experimental buckling loads to the analytical buckling loads using equations 2.9, 2.10, and 2.15 developed by Zureick and Steffen (2000) were used in this investigation.

2.2 CONCENTRIC COLUMNS (LOCAL BUCKLING)

Yoon (1993) investigated experimentally and analytically short-term compression behavior for axially loaded I-shaped FRP columns. He tested a total of thirty-two I-shaped columns made from pultruded fiber reinforced polymer materials, twenty-two specimens made using a polyester matrix, and ten specimens made using a vinylester matrix. The sizes and lengths for these

specimens were selected so that local buckling occurred at loads less than those which would cause global buckling or material failure. The lengths varied from 35 in to 120 in, with slenderness ratios ranging from 20 to 50. The width to thickness ratios of the flange ranged from 6 to 13, and the depth to thickness ratios for the web ranged from 15 to 26. The experiment was terminated at the post buckling stage. After applying the load, the column specimen was observed until out-of-plane deflections at the tips of the flange occurred. Critical buckling loads were experimentally determined and compared to the analytical critical buckling loads.

An analytical solution was developed for the prediction of the local buckling loads for pultruded columns composed of flat plates under short-term axial loads. The proposed solution was based on classical orthotropic plate theory. It accounts for the rotational restraint at the junction of the web and the flange.

$$\sigma_{cr} = \frac{\pi^2 \sqrt{E_{11} E_{22}}}{12\,(1-\nu_{12}\nu_{21})(b/t)^2} \tag{2.16}$$

where,

σ_{cr} : the critical buckling stress.

E_{11} : major Young's modulus.

E_{22} :minor Young's modulus.

ν_{12} : major Poisson's ratio, $|\nu_{12}| < \sqrt{\frac{E_{11}}{E_{22}}}$.

ν_{21} : minor Poisson's ratio, $|\nu_{21}| < \sqrt{\frac{E_{22}}{E_{11}}}$.

t: the thickness of the plate.

b: the width of the plate or half the with of the flange.

Tension and compression tests were performed to estimate the material properties E_{11}, E_{22}, ν_{12}, and ν_{21}. The average values for E_{11} and E_{22} in tension and compression tests were almost identical. The experimental local buckling loads ($P_{\exp}$) were compared to those predicted theoretically (P_{pred}) using equations 2.16. The ratios of the experimental local buckling loads to the analytical local buckling loads using equations 2.16 developed by Yoon (1993) were used in this investigation.

Tomblin and Barbero (1994) investigated local flange buckling for FRP thin-walled pultruded columns. Wide flange FRP I-shaped columns were used in this investigation. Local buckling tests were performed on 4 in. x 4 in. x ¼ in., 6 in. x 6 in. x ¼ in., 6 in. x 6 in. x 3/8 in., and 8 in. x 8 in. x 3/8 in. cross-sections. Sothwell's method was used to reduce the data and determine the critical loads (Southwell, 1932). For mode II (the shortest lengths), the percentage difference between the experimental and the theoretical was less than 11 percent. For mode III (the intermediate length), all percentage differences between the experimental and the theoretical were less than 9 percent, and all loads were slightly less than the theoretical values. For mode IV (the longest column lengths), all percentage differences were 13-24 percent, and all loads were below the theoretical ones. The local buckling loads obtained experimentally were in good agreement with the theoretical predictions. Tomblin and Barbero (1994) did not provide results that

could be used in this study.

2.3 BEAMS

Stoddard (1997) investigated experimentally and analytically lateral-torsional behavior of hybrid (E-glass and carbon fiber) and non-hybrid (all glass fiber) FRP I-shaped beams subjected to vertical concentrated short term loading acting at mid-spans. Five different I-shaped 4 x 2 x ¼ in. reinforced cross sections were tested. Eight specimens were used in this study. Elastic lateral-torsional buckling of doubly symmetric FRP beams was predicted theoretically using three approaches.

Three analytical approaches were presented to calculate the lateral-torsional buckling loads. The first approach is the classical one-dimensional isotropic theory derived by Timosheko and Gere (1961) for thin walled slender I-shapes loaded with pure moment around the X-axis. The isotropic material properties were replaced by orthotropic material properties. The second approach uses the energy method along with an orthotropic constitutive system developed by Pandey at. al (1995). This approach failed to account for the importance of load height above the shear center and bending-twisting coupling effects. The third approach was derived to account for these deficiencies in order to predict more accurately the lateral-torsional buckling loads for FRP beams. The approximate solution for the critical lateral-torsional buckling load using the third approach was derived to be:

$$P_{cr} = \frac{17.199}{L^2}\sqrt{GJ.I_{yy}}\left[\sqrt{1+\frac{\pi^2 I_{\omega\omega}}{L^2 GJ}+2.989\frac{\alpha_{sc}^2 I_{yy}}{L^2 GJ}-0.176\frac{H_s^2}{GJ.I_{yy}}}+1.729\frac{\alpha_{sc}}{L}\sqrt{\frac{I_{yy}}{GJ}}\right] \quad (2.17)$$

where,

P_{cr} : critical load.

L: span length.

G: shear modulus of elasticity.

J: torsional constant.

I_{yy} : minor axis bending stiffness, $E_{a,Y}.I_Y$.

I_Y : minor axis second moment of inertia.

$E_{a,Y}$: apparent modulus of elasticity in minor axis.

$I_{\omega\omega}$: wraping stiffness, $E_{a,Y}.C_\omega$.

C_ω : wraping constant.

α_{sc} : distance between shear center and application of load.

H_s : bending-twisting coupling term.

Tension and compression tests were conducted to determine the material properties. Experimental results for lateral-torsional buckling loads were compared to the analytical results. Results developed by Stoddard (1997) were used in this investigation.

Brooks and Turvey (1995b) tested only one FRP I-shape specimen twice at three different span lengths ranging from1750 mm to 1250 mm in the first set of buckling. Load was always applied through the centroid of the specimen. Turvey (1996a) performed a second set of buckling tests. An identical I-shape FRP section was used with three different span lengths ranging from 1500 mm to 500 mm with the load applied at, below, and above the centroid.

In the first set of tests, the experimental results were compared with two lateral-torsional buckling theories developed for isotropic materials. The first formula was derived by Nethercot (1973). It consisted of a buckling coefficient, a material parameter, and slenderness ratio components. The second formula was developed by Timoshenko and Gere (1961) using the energy method. The formula is used for loading a cantilever beam through its centroidal axis. Brooks and Turvey (1995b) evaluated these equations at appropriate span lengths by substituting the orthotropic properties for the isotropic material constants. The results showed that these formulas are not consistent, particularly at shorter spans. The errors ranged from 16.6% to 15.5%.

In the second set of tests, the effect of load position, below or above the centroid on lateral-torsional buckling of FRP I-shape cantilever beams, was examined (Turvey, 1996a). The experimental results of buckling moments were compared to a modified formula for theoretical critical moments that account for load position predicted by Nethercot's (1973). The theoretical closed form solution underestimates the experimental buckling loads by 55%. Turvey and Brooks (1995a and 1996a) concluded that if out-of-straightness and pre-buckling deformations were accounted for in the theoretical predictions, the theoretical results would be better. Brooks and Turvey (1995a, 1995b, and 1996a) did not provide enough data points to be used in this study.

Davalos et al. (1997) conducted a comprehensive experimental and analytical analysis to investigate flexural-torsional buckling for two full-size pultruded FRP I-beams under mid-span concentrated loads. The theoretical

analysis is based on energy principles. The total potential energy equations governing instability for the I-beams were developed using nonlinear plate theory. The Rayleigh Ritz method was used to solve the equilibrium equation. The experimental critical bucking loads were compared to the proposed analytical solutions and finite-element analysis results. A good agreement was obtained, however Davalos et al. (1997) did not provide enough data points to be used in this investigation.

CHAPTER 3

STATISTICAL PROPERTIES

3.1 DISTRIBUTIONS CONSIDERED

The determination of the statistics and probability distributions of the random variables describing material properties plays an important role in the development of probabilistic based design specifications. The choice of the probability distribution to represent the material property data will have a large effect on the calculated reliability. Assuming different distributions for the material properties can result in computed probabilities of failure that vary by more than an order of magnitude.

Normal, Lognormal, and Weibull distributions have been investigated. Several approaches have been used for the distribution problem. The steel industry prescribed a lognormal distribution for steel material properties. The wood industry prescribed a Weibull distribution. The Military Handbook examines the two-parameter Weibull distribution first. If it is not rejected, no further distribution is examined. If it is rejected, normal and lognormal distributions are examined (MIL-HDBK-17, 1990).

The determination of the nominal material property and the reliability analysis to determine resistance factors will be affected by the chosen probability distribution. The performance of the distribution tails most affect civil engineering applications. Distributions that are similar in the central regions can have different behavior in the tail regions of the data. Civil engineers are interested in lower tails of probability distributions for strengths. The lower tails

of Wiebull, normal and lognormal probability distributions are shown in figure1.

A special case of the three-parameter Weibull cumulative distribution is the two-parameter Weibull cumulative distribution. The two-parameter Weibull cumulative distribution function is as follows:

$$F_x(x) = 1 - \exp\left[-\left(\frac{x}{\alpha}\right)^k\right] \tag{3.1}$$

where:

k: the shape parameter.

α: the scale parameter.

The shape parameter is determined by solving the following equation numerically.

$$\frac{n}{k} + \sum_{i=1}^{n} \ln x_i - \frac{n}{\sum_{i=1}^{n} x_i^k} \sum_{i=1}^{n} x_i^k \ln x_i = 0 \tag{3.2}$$

where:

n: the number of data points.

The scale parameter is determined from the following formula:

$$\alpha = \left(\frac{\sum_{i=1}^{n} x_i^k}{n}\right)^{\frac{1}{k}} \tag{3.3}$$

For normal distribution, the probability that a data point falls between a and b is given by the area under the function:

$$\text{f(x)} = \frac{1}{\sigma\sqrt{2\pi}} e^{-(x-\mu)^2/2\sigma^2} \tag{3.4}$$

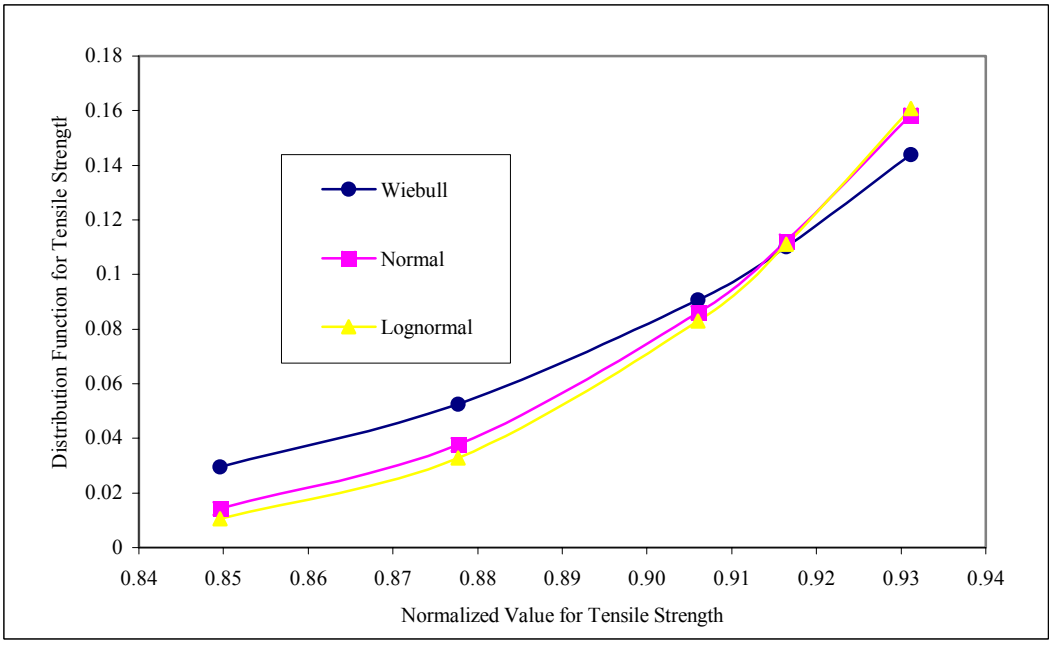

Figure 1. Lower Tail of Cumulative Distribution Functions.

For lognormal distribution, the probability that a data point falls between a and b is given by the area under the function:

$$f(x)= \frac{1}{x\sigma\sqrt{2\pi}} e^{-[\log(x)-\mu]^2/2\sigma^2} \qquad (3.5)$$

where:

x: the data point.

μ: the mean for $\ln x_i$.

σ: the standard deviation of $\ln x_i$.

3.2 DISTRIBUTION FITTING

Strength, modulus of elasticity, and ultimate strain were determined for tension, compression, flexure, and shear loadings. Data used in this study are

taken from two different studies that examined the short-term axial compressive strength of E-glass/vinylester pultruded I- and box-shaped components (Zureick, 1997), and the short-term eccentric axial compressive strength of E-glass/polyester pultruded square tube components (Kang, 2000). Coupons from the former study are labeled VG. Coupons from the later study are labeled T for the tension test, C for the compression test, V for the shear test, and B for the flexure test. Weibull, normal and lognormal distributions were considered. The Anderson-Darling test was used to examine the data. The observed significance level (OSL) is the probability to determine the value of the test statistic at least as large as that determined from the data set if the hypothesis that the data set is actually from the distribution being examined is true. Usually, if the OSL is less than 0.05, the null hypothesis is rejected. For different data sets, the OSL of the three distributions were calculated and shown in table 1. Given in table 1, bold font represents OSL > 0.05 and underline font represents the highest value of OSL for each data set. For the cases described in table 1, lognormal distribution is the best distribution for strength. Weibull or lognormal distributions are the best distributions for modulus of elasticity. Normal distribution is the most appropriate distribution for ultimate strain. The FRP material properties were considered to follow a two-parameter Weibull distribution. The Weibull distribution has been the most common probability distribution to be used with FRP material properties (King, 1986, Rust et al., 1989). A three-parameter Weibull distribution has sometimes been used, but it has been shown that the two-parameter Weibull distribution is adequate (Alqam, 2002). It is assumed that the nominal FRP

Table 1. OSL of the Three Distributions for Strength, Modulus of Elasticity, and Ultimate Strain with Tension, Compression, Flexure, and Shear.

Property	Observed Significance Level (OSL)			
	N	Weibull	Normal	Lognormal
Longitudinal Tensile Strength (F_t)				
VG 1 - 6	30	0.009	**0.113**	**0.195**
VG 7 - 12	30	**0.302**	**0.198**	**0.120**
VG 13 - 18	24	**0.136**	**0.142**	**0.147**
VG 19 - 24	24	0.008	**0.142**	**0.260**
T	30	**0.407**	**0.757**	**0.684**
Longitudinal Compressive Strength (F_c)				
VG 1 - 6	30	0.001	**0.064**	**0.154**
VG 7 - 12	30	**0.213**	**0.576**	**0.662**
VG 13 - 18	24	**0.088**	**0.106**	**0.117**
VG 19 - 24	24	**0.469**	**0.542**	**0.467**
C	30	**0.213**	**0.147**	**0.106**
Longitudinal Flexural Strength (F_b)				
B	30	**0.060**	**0.242**	**0.313**
Shear Strength (F_v)				
VG 19 - 24	24	**0.517**	**0.204**	**0.103**
V	18	**0.068**	**0.195**	**0.275**
Longitudinal Tensile Modulus (E_t)				
VG 1 - 6	30	**0.179**	**0.500**	**0.517**
VG 7 - 12	30	0.022	0.001	0.000
VG 13 - 18	24	0.01	0.012	0.012
VG 19 - 24	24	**0.171**	**0.519**	**0.546**
T	30	**0.171**	**0.372**	**0.379**
Longitudinal Compressive Modulus (E_c)				
VG 1 - 6	30	**0.154**	**0.333**	**0.361**
VG 7 - 12	30	**0.053**	0.006	0.002
VG 13 - 18	24	0.01	0.012	0.015
VG 19 - 24	24	**0.299**	**0.199**	**0.174**
C	30	**0.499**	**0.587**	**0.563**
Longitudinal Flexural Modulus (E_b)				
B	30	**0.412**	**0.560**	**0.472**
Shear Modulus (G_v)				
VG 19 - 24	24	**0.065**	**0.297**	**0.350**
V	18	**0.111**	**0.320**	**0.473**
Ultimate Tensile Strain (ε_{ut})				
T	30	**0.085**	**0.553**	**0.537**
Ultimate Compressive Strain (ε_{uc})				
C	13	**0.110**	**0.334**	**0.472**
Ultimate Flexural Strain (ε_{ub})				
B	30	**0.092**	**0.500**	**0.516**
Ultimate Shear Strain (γ_v)				
V	18	0.047	0.038	0.016

design properties would be the five-percentile value. The five-percentile value is typical for civil engineering applications and appropriate for FRP materials (McNutt, 1998; Ellingwood, 2000).

The OSL for the Weibull distribution (MIL-HDBK-17, 1990):

$$OSL = 1/\{1 + \exp[-0.10 + 1.24\ln(AD^*) + 4.54\ AD^*]\} \tag{3.6}$$

where:

$$AD^* = \left(1 + \frac{0.2}{\sqrt{n}}\right) AD \tag{3.7}$$

$$AD = \sum_{i=1}^{n} \frac{1-2i}{n}[1 - \exp(z_{(i)})] - z_{(n+1-i)} - n \tag{3.8}$$

$$z_{(i)} = [x_{(i)}/\alpha]^k, \qquad \text{for i = 1,…,n} \tag{3.9}$$

The OSL for the normal and the lognormal distributions (MIL-HDBK-17, 1990):

$$OSL = 1/\{1 + \exp[-0.48 + 0.78\ln(AD^*) \_ 4.58\ AD^*]\} \tag{3.10}$$

where:

$$AD^* = \left(1 + \frac{4}{n} - \frac{25}{n^2}\right) AD \tag{3.11}$$

$$\text{AD} = \sum_{i=1}^{n} \frac{1-2i}{n}\{\ln[F_0(z_{(i)})] + \ln[1 - f_0(z_{(n+1-i)})]\} - n \tag{3.12}$$

For the normal distribution is:

$$z_{(i)} = \frac{x_{(i)} - \mu}{\sigma}, \text{ for i = 1,…,n} \tag{3.13}$$

For the lognormal distribution is:

$$z_{(i)} = \frac{\ln(x_{(i)}) - \mu}{\sigma}, \text{ for i = 1,…,n} \tag{3.14}$$

3.3 CORRELATION BETWEEN VARIABLES

The correlation coefficient provides a measure of the linear relationship between two variables. The correlation coefficient, ρ, between two sets of data is obtained from the following formula:

$$\rho = \frac{\frac{1}{n}\sum_{i=1}^{n}(x_i - \mu_x)(y_i - \mu_y)}{\sigma_x \sigma_y} \tag{3.15}$$

where:

x_i : data point in the first data set.

y_i : data point in the second data set.

μ_x : the mean for the first data set.

μ_y : the mean for the second data set.

σ_x : the standard deviation for the first data set.

σ_y : the standard deviation for the second data set.

Sachs (1984) presented a test procedure to examine the presence of the correlation coefficients. The computed correlation coefficient is compared with the value computed from the formula:

$$r = t_{n-2;\alpha} / \sqrt{(n-2) + t_{n-2;\alpha}^2} \tag{3.16}$$

where,

$t_{n-2;\alpha}$: percentage point for the t-distribution.

n: sample size.

(n-2): degrees of freedom.

α: level of significant.

The correlation coefficients between strength and modulus of elasticity, strength and ultimate strain, modulus of elasticity and ultimate strain were calculated and given in table 2. These values were tested by comparing them to the values from equation 3.16 (Sachs, 1984) for two sided test at 5% level with degrees of freedom equal to number of data points minus two (DF=n-2). For n=30, the corresponding value is 0.361. For n=24, the corresponding value is 0.404. For n=18, the corresponding value is 0.468. For n=13, the corresponding value is 0.553. It is noticed that 9 out of 13 correlation factors for modulus of elasticity versus strength (tension, compression, bending and shear) pass the corresponding values, which means they have strong positive linear relationships. For modulus of elasticity versus ultimate strain, 2 out of 4 have negative strong linear relationships. For strength versus ultimate strain, 1 out of 4 has a negative strong linear relationship.

Table 2. Correlation Coefficients between Strength and Modulus of Elasticity, Strength and Ultimate Strain, Modulus of Elasticity and Ultimate Strain.

Correlation Coefficient	T (N=30)	C (N=30)	B (N=30)	V (N=18)	VG 1-6 (N=30)	VG 7-12 (N=30)	VG 13-18 (N=24)	VG 19-24 (N=24)
E_{tl}, F_{tl}	0.791				0.680	0.770	0.730	0.080
E_{tl}, ε_{ut}	-0.438							
F_{tl}, ε_{ut}	0.155							
E_{cl}, F_{cl}		0.281			0.400	0.730	0.750	0.290
E_{cl}, ε_{uc}		-0.328						
F_{cl}, ε_{uc}		-0.596						
E_{bl}, F_{bl}			0.826					
E_{bl}, ε_{ub}			-0.445					
F_{bl}, ε_{ub}			0.029					
G_v, F_v				0.650				0.370
G_v, γ_u				0.025				
F_v, γ_u				0.451				

CHAPTER 4

THREE-PARAMETER VS. TWO-PARAMETER WEIBULL DISTRIBUTION FOR PULTRUDED COMPOSITE MATERIAL PROPERTIES

This chapter is a slightly revised version of a paper published in the journal, Composite Structures, in 2002 by Maha Alqam, Richard M. Bennett, and Abdul-Hamid Zureick:

Alqam, M., Bennett, R. M., and Zureick, A-H. (2002). "Three-parameter vs. two-parameter Weibull distribution for pultruded composite material properties." Composite Structures, Vol. 58, 497-503.

My primary contribution to the paper is comparing three-parameter vs. two-parameter Weibull distributions on the basis of goodness of fit, nominal design values, and allowable load to achieve uniform reliability.

4.1 ABSTRACT

The three-parameter and two-parameter Weibull distributions are compared using 26 mechanical property data sets of fiber-reinforced polymeric (FRP) composite materials manufactured by the pultrusion process. Both strength and stiffness properties were examined. The probability distributions were compared on the basis of goodness of fit, nominal design values, and allowable load to achieve uniform reliability. It is recommended that the two-parameter Weibull distribution be used to characterize FRP composite material properties. The primary bases for this recommendation are small differences in nominal design values and small differences in allowable loads between the two-parameter and three-parameter Weibull distributions. Other supporting reasons for the recommendation are similar observed significance levels in distribution fitting,

computational efficiency, and the fact that the location parameter of the three-parameter Weibull distribution is near the first order statistic.

4.2 INTRODUCTION

The determination of the statistics and probability distributions of the random variables describing material properties plays an important role in the development of probabilistic based design specifications. The choice of the probability distribution chosen to represent the material property data will have a large effect on the calculated reliability. Assuming different distributions for the material properties can result in computed probabilities of failure that vary by more than an order of magnitude. This is the result of the lower tail behavior of different cumulative distribution functions, which has become known as the tail-sensitivity problem in structural reliability (Ditlevsen, 1981).

The Weibull distribution (Weibull, 1951) is often used to describe the strength of fiber-reinforced polymer (FRP) composites (King, 1986, Rust et al., 1989). Typically, the two-parameter Weibull distribution is used, although the three-parameter Weibull distribution is more robust and may provide a better characterization of the data. While the two-parameter Weibull distribution was previously used by Mottram (1994) to examine the compressive strength property data of flat pultruded panels, the three-parameter Weibull distribution was used by Abdallah et al. (1996) to assess the reliability of glass-fiber reinforced polymeric pultruded rods and by Zureick and Steffen (2000) to compute the 95% lower confidence limit on the 5^{th} percentile of the compressive property data of E-glass polyester and vinylester pultruded single angles.

This paper examines the two-parameter versus the three-parameter Weibull distribution for characterizing FRP composite material properties. Only the Weibull distributions are considered in this paper, although other probability distributions may also fit the data. The purpose of the paper is to determine the adequacy of the two-parameter Weibull distribution or if there is justification for using the three-parameter Weibull distribution for FRP material properties.

The three-parameter Weibull cumulative distribution function is given by:

$$F_X(x) = 1 - \exp\left[-\left(\frac{x-\delta}{\theta}\right)^{\beta}\right] \qquad x \geq \delta \qquad (4.1)$$

in which θ is the scale parameter, β is the shape parameter, and δ is the location parameter. If $\delta=0$, the distribution becomes the two-parameter Weibull distribution.

Zanakis (1979) documents seventeen different methods for obtaining the parameters of the three-parameter Weibull distribution. Two common parameter estimation methods used in engineering are the modified moment method and the maximum likelihood method, with those being the methods considered in this paper. The two-parameter and three-parameter Weibull distributions are compared on the basis of the goodness-of-fit of the distribution to FRP material property data and lower tail behavior. The lower tail behavior is examined through the analysis of nominal design values and probabilistic based allowable loads.

Data used for the comparisons are taken from two different studies that examined the short-term axial compressive strength of E-glass/vinylester

pultruded I- and box-shaped components in one case (Zureick and Scott, 1997), and the short-term eccentric axial compressive strength of E-glass/polyester pultruded box-shaped components in another case (Zureick et al, 2001). Coupons from the former and latter study are labeled VG and PG, respectively. Coupon data from a study (Mottram, 1994) of E-glass/polyester plates is also included in this study, and labeled as PG-M. Both stiffness and strength parameters are examined, with a total of twenty-six data sets and over seven hundred data points being considered. A summary of the data sets is given in Table 3, which gives the sample size and coefficient of variation of each data set.

4.3 PARAMETER ESTIMATION

Two methods are used for parameter estimation, the modified moment method and the maximum likelihood method. Moment methods are based on equating sample moments to the corresponding distribution moments. The mean value or the first moment, μ, of the Weibull distribution is:

$$\mu = \delta + \theta\Gamma\left(1 + \frac{1}{\beta}\right) \tag{4.2}$$

where Γ is the gamma function. The variance or second moment about the mean, σ^2, is:

$$\sigma^2 = \theta^2\left[\Gamma\left(1 + \frac{2}{\beta}\right) - \Gamma^2\left(1 + \frac{1}{\beta}\right)\right] \tag{4.3}$$

By equating the mean μ to the sample mean $\bar{x}$ and the variance σ^2 to the sample variance s^2, equations 4.2 and 4.3 can be used to estimate the parameters of the Weibull distribution. An estimate of the location parameter, δ, is also required,

with a common estimate for δ being x_1, the first order statistic (the first data point when ordering from smallest to largest). A better estimate of the location parameter is (Zanakis, 1979):

$$\hat{\delta} = \frac{x_1 x_n - x_2^2}{x_1 + x_n - 2x_2} \tag{4.4}$$

in which $\hat{\delta}$ is the estimate of the location parameter, δ, and x_i is the i^{th} order statistic of the sample of size n.

Improvements have been made to the basic moment method, resulting in the modified moment method (Dodson, 1994). Parameters of the Weibull distribution are estimated from the following equations:

$$\frac{s^2}{(\bar{x} - x_1)^2} = \frac{\Gamma\left(1 + \frac{2}{\hat{\beta}}\right) - \Gamma^2\left(1 + \frac{1}{\hat{\beta}}\right)}{\left[\left(1 - n^{-1/\hat{\beta}}\right)\Gamma\left(1 + \frac{1}{\hat{\beta}}\right)\right]^2} \tag{4.5}$$

$$\hat{\theta} = \frac{s}{\sqrt{\Gamma\left(1 + \frac{2}{\hat{\beta}}\right) - \Gamma^2\left(1 + \frac{1}{\hat{\beta}}\right)}} \tag{4.6}$$

$$\hat{\delta} = \bar{x} - \hat{\theta}\Gamma\left(1 + \frac{1}{\hat{\beta}}\right) \tag{4.7}$$

in which a hat indicates the estimate of the parameter. Equations 4.5 – 4.7 will be used in this paper as one estimate of the parameters of the three-parameter Weibull distribution.

In two cases out of the 26 data sets examined, the modified moment method resulted in a location parameter less than zero. In these two cases, the

location parameter was set to zero as a negative location parameter would imply the possibility of negative values for the material properties. For cases in which there was a positive estimate of the location parameter ($\hat{\delta}$), the average values of $\hat{\delta}/x_1$ and $\hat{\delta}/\bar{x}$ are 0.90 and 0.77, respectively, where x_1 and $\bar{x}$ are the minimum (first order statistic) and sample mean of the data set. Values of the location parameter in terms of the first order statistic and the mean value are given in Table 3.

The second method of estimating the parameters of the Weibull distribution that will be used is the maximum likelihood method. This method requires solving the following simultaneous equations (Dodson, 1994).

$$\left(\sum_{i=1}^{n}(x_i-\hat{\delta})^{\hat{\beta}}\ln(x_i-\hat{\delta})\right)\left(\sum_{i=1}^{n}(x_i-\hat{\delta})^{\hat{\beta}}\right)^{-1}-\left(\frac{1}{\hat{\beta}}\right)-\sum_{i=1}^{n}\ln(x_i-\hat{\delta})/n=0 \tag{4.8}$$

$$\hat{\theta}=\left(\frac{\sum_{i=1}^{n}(x_i-\hat{\delta})^{\beta}}{n}\right)^{\frac{1}{\hat{\beta}}} \tag{4.9}$$

$$\frac{\hat{\beta}}{\hat{\theta}^{\hat{\beta}}}\sum_{i=1}^{n}(x_i-\hat{\delta})^{\hat{\beta}-1}-(\hat{\beta}-1)\sum_{i=1}^{n}(x_i-\hat{\delta})^{-1}=0 \tag{4.10}$$

Equation 4.10 can be difficult to solve. This is apparent from the graph shown in Figure 2, in which the left hand side of Equation 4.10 is plotted for different values of $\hat{\delta}$ for the longitudinal tensile strength of data set VG19-24. The values of $\hat{\theta}$ and $\hat{\beta}$ are held constant and equal to the maximum likelihood estimate ($\hat{\theta}=58.7$ Mpa and $\hat{\beta}=2.18$) while $\hat{\delta}$ is varied. The change in

Table 3. Description of Data Sets and Location Parameter for Three-Parameter Weibull Distribution of $\hat{\delta}/x_1$ and $\hat{\delta}/\bar{x}$.

Material Property (1)	Sample Size (2)	Coefficient of Variation (3)	Location Parameter, $\hat{\delta}$			
			Modified Moment Method		Maximum Likelihood Method	
			$\hat{\delta}/x_1$ (4)	$\hat{\delta}/\bar{x}$ (5)	$\hat{\delta}/x_1$ (6)	$\hat{\delta}/\bar{x}$ (7)
Longitudinal Tensile Strength						
VG 1-6	30	0.074	0.984	0.883	0.996	0.894
VG 7-12	30	0.130	0.949	0.760	0.925	0.741
VG 13-18	24	0.102	0.957	0.811	0.983	0.833
VG 19-24	24	0.077	0.913	0.786	0.979	0.843
PG	30	0.069	0.800	0.680	0.878	0.746
Longitudinal Compressive Strength						
VG 1-6						
VG 7-12	30	0.073	0.985	0.886	0.994	0.894
VG 13-18	30	0.093	0.756	0.605	0.932	0.747
VG 19-24	24	0.114	0.969	0.819	0.995	0.841
PG	24	0.106	0.948	0.793	0.940	0.786
PG-M	30	0.122	0.935	0.750	0.938	0.752
	51	0.092	0.560	0.427	0.819	0.624
Shear Strength						
VG 19-24	24	0.072	0*	0*	0*	0*
PG	18	0.098	0.950	0.816	0.988	0.848
Transverse Compressive Strength						
PG-M	52	0.060	0.974	0.871	0.982	0.877
Longitudinal Tensile Modulus						
VG 1-6	30	0.068	0.949	0.836	0.938	0.826
VG 7-12	30	0.096	0*	0*	0*	0*
VG 13-18	24	0.116	0.917	0.742	0.962	0.778
VG 19-24	24	0.046	0.974	0.902	0.981	0.908
PG	30	0.063	0.947	0.839	0.947	0.838
Longitudinal Compressive Modulus						
VG 1-6						
VG 7-12	30	0.054	0.940	0.843	0.973	0.873
VG 13-18	30	0.087	0.852	0.703	0*	0*
VG 19-24	24	0.132	0.940	0.753	0.984	0.788
PG	23	0.040	0.749	0.682	0*	0*
	30	0.040	0.941	0.864	0.962	0.884
Shear Modulus						
VG 19-24	24	0.113	0.841	0.666	0*	0*
PG	18	0.104	0.895	0.742	0.970	0.804

* indicates location parameter was set equal to zero

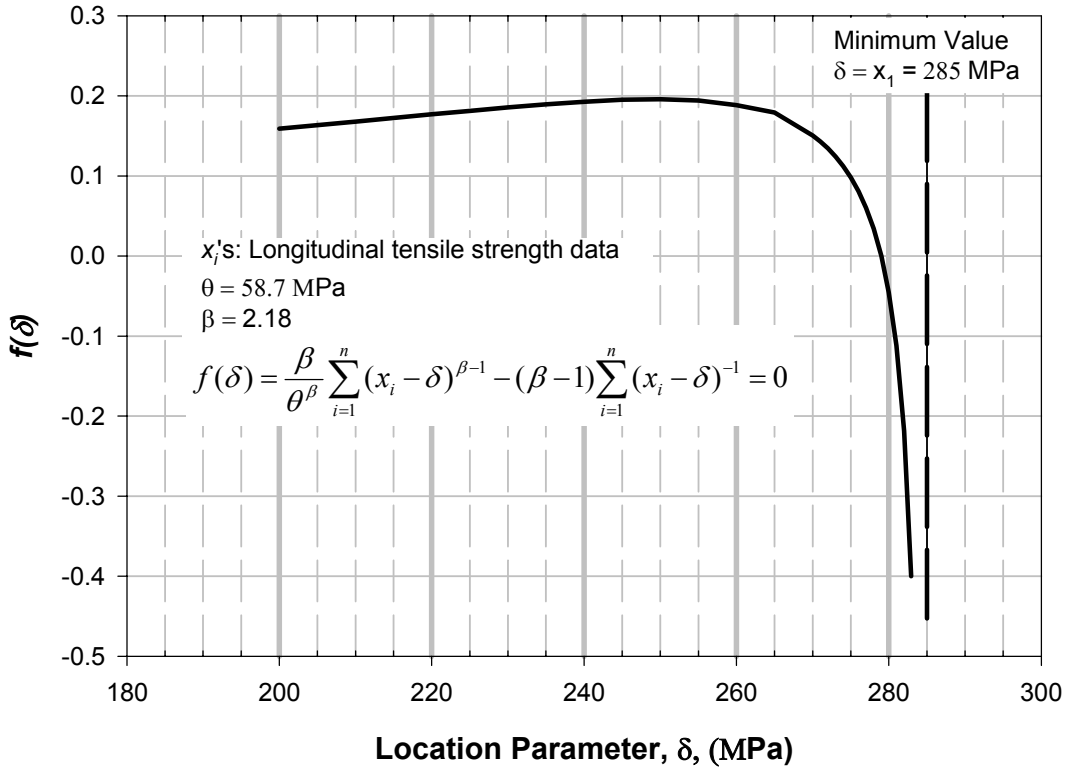

Figure 2. Value of Equation 4.10 vs. Location Parameter, δ

curvature near the root may cause many standard root-finding techniques, such as Newton-Raphson, to fail. Even if the method does not fail, the flat slope for most of the graph coupled with the steep slope near the root often results in slow convergence. The best technique is generally to start with a value just slightly less than the minimum data point, reduce this value until there is a change in sign, and then use some standard root finding technique over the interval in which the sign changes.

In five out of the 26 data sets examined, the maximum likelihood estimator of the location parameter was less than zero. Often in these cases, the estimators were unreasonable. For example, the maximum likelihood estimate of

the location parameter for the longitudinal tensile modulus for specimens VG7-12 was negative approximately eight times the mean value. The shape parameter was 139.5, while the typical range of the shape parameter is 6 to 25. In these five cases, the location parameter was taken as zero, or the two-parameter Weibull distribution was used.

The maximum likelihood estimator of the location parameter is generally just slightly less than the minimum data point. For the 19 cases with a positive location parameter, the average values of $\hat{\delta}/x_1$ and $\hat{\delta}/\bar{x}$ are 0.96 and 0.82, respectively. The location parameter from the maximum likelihood method is given in Table 3.

4.4 GOODNESS OF FIT

Many methods, such as Chi-square, the Kolmogorov-Smirnov, exist for determining the goodness of fit of a probability distribution to a set of data. The Anderson-Darling test was chosen for this study as it is more sensitive to the tail behavior (Lawless, 1982), and has been recommended for statistical analysis of composites (Rust et al., 1989). The sensitivity to the tail behavior is particularly useful in structural engineering applications, where the tail is important in computing the structural reliability. The Anderson-Darling statistic is obtained as:

$$A_n^2 = n\int_{-\infty}^{\infty} \frac{\left[\widetilde{F}_n(x) - F_0(x)\right]^2}{F_0(x)\left[1 - F_0(x)\right]} dF_0(x) \tag{4.11}$$

in which $\widetilde{F}_n(x)$ is a step function that jumps at the order statistics of x, and

$F_0(x)$ is the hypothesized continuous cumulative distribution function. The Anderson-Darling statistic is a measure of the square of the error between the data and the hypothesized distribution weighted so that the tails of the data are more important than the central portion. For computation purposes, the Anderson-Darling statistic can be obtained as:

$$A_n^2 = \sum_{i=1}^{n}\left[\frac{1-2i}{n}\left\{\ln\left[F_0\left(x_{(i)}\right)\right]+\ln\left[1-F_0\left(x_{(n+1-i)}\right)\right]\right\}\right]-n \tag{4.12}$$

in which $x_{(i)}$ is the i^{th} order statistic of the data set. For the Weibull distribution, an observed significance level, OSL, is obtained as follows (Rust et al, 1989):

$$OSL = \frac{1}{1+\exp\left[-0.10+1.24\ln AD^* + 4.48 AD^*\right]} \tag{4.13}$$

in which

$$AD^* = \left[1+\frac{0.2}{\sqrt{n}}\right]A_n^2 \tag{4.14}$$

The OSL is the probability of obtaining a value of the test statistic at least as large as that obtained from the data if the hypothesis that the data are actually from the distribution being tested is true. Typically, a 5% significance level is used, so that the null hypothesis is only rejected if the OSL is less than 0.05.

The modified moment method and the maximum likelihood method were used to determine parameters of the three-parameter Weibull distribution for each of the 26 data sets being considered in this paper. The maximum likelihood method was also used to determine parameters for the two-parameter Weibull distribution by setting $\delta=0$ and only using equations 4.8 and 4.9. Although the

parameters for the two-parameter Weibull distribution could be determined using moment methods, the maximum likelihood method is the generally used method for the two-parameter Weibull distribution (Rust et al., 1989). An OSL was obtained for each of the distributions for each data set. The results are shown in Table 4.

The two-parameter Weibull distribution cannot be rejected at the 5% significance in nineteen out the 26 cases. The three-parameter Weibull distribution is rejected in five cases for parameters determined with the modified moment method and in three cases for parameters determined with the maximum likelihood method. In most cases in which the three-parameter Weibull was rejected, the two-parameter Weibull was also rejected for the same data set.

The average OSL for the two-parameter Weibull distribution was 0.178, with the average OSL for the three-parameter Weibull distribution being 0.386 and 0.356 for the modified moment method and the maximum likelihood method, respectively. Although strictly speaking the OSL cannot be used for ranking distributions, higher values of the OSL do indicate a higher significance level. Therefore, it appears that the three-parameter Weibull distribution is slightly preferable to the two-parameter Weibull distribution, though the two-parameter Weibull distribution cannot be rejected in most cases.

Abdallah et al. (1996) compared the two-parameter and three-parameter Weibull distribution for compressive, tensile, and flexural strength and stiffness of glass fiber reinforced pultruded rods. Distributional parameters were obtained by

Table 4. Observed Significance Level Using the Anderson-Darling Test for Different Weibull Distributions.

Material Property (1)	Observed Significance Level		
		Three-parameter Weibull	
	Two-parameter Weibull (2)	Modified Moment Method (3)	Maximum Likelihood Method (4)
Longitudinal Tensile Strength			
VG 1-6	0.009	0.823	0.817
VG 7-12	0.302	0.045	0.072
VG 13-18	0.138	0.224	0.146
VG 19-24	0.008	0.208	0.420
PG	0.699	0.871	0.860
Longitudinal Compressive Strength			
VG 1-6	0.001	0.536	0.320
VG 7-12	0.212	0.475	0.727
VG 13-18	0.088	0.183	0.117
VG 19-24	0.469	0.272	0.303
PG	0.214	0.131	0.096
PG-M	0.122	0.255	0.157
Shear Strength			
VG 19-24	0.517	0.610*	0.517*
PG	0.073	0.544	0.486
Transverse Compressive Strength			
PG-M	0.020	0.546	0.424
Longitudinal Tensile Modulus			
VG 1-6	0.179	0.505	0.522
VG 7-12	0.022	0.030*	0.022*
VG 13-18	0.010	0.023	0.012
VG 19-24	0.177	0.622	0.508
PG	0.180	0.504	0.414
Longitudinal Compressive Modulus			
VG 1-6			
VG 7-12	0.153	0.518	0.483
VG 13-18	0.052	0.012	0.052*
VG 19-24	0.010	0.042	0.036
PG	0.299	0.386	0.299*
	0.504	0.753	0.678
Shear Modulus			
VG 19-24	0.065	0.312	0.065*
PG	0.116	0.598	0.701

* indicates a location parameter of 0.0

using linear regression of the data when plotted on Weibull probability paper. The two-parameter and three-parameter Weibull distributions were compared on the basis of the correlation coefficient between the best fit line and the data. The correlation coefficient for the two-parameter Weibull distribution averaged 0.902 for the 22 data sets considered, while the correlation coefficient averaged 0.924 for the three-parameter Weibull distribution. This is consistent with the present results in that the three-parameter Weibull distribution in general provides a slightly better fit of the data than the two-parameter Weibull distribution, although the two-parameter Weibull distribution provides a reasonable fit.

4.5 NOMINAL DESIGN VALUE

Nominal design values are used in design practice. Typically in structural engineering, the nominal design value for material properties is the 5-percentile value (Ellingwood, 2000). The 5-percentile value for each of the three Weibull distributions being considered is shown in Table 5. Statistical uncertainty, or the uncertainty from using a finite sample size to estimate the parameters, was not accounted for in any of the design values. Several methods are available for accounting for statistical uncertainty, with no agreed upon method. Rather than potentially biasing the results by accounting for statistical uncertainty, it was not included in the calculations, although it would need to be included in actual code development.

The three-parameter Weibull distributions resulted in 5-percentile values that averaged five percent greater than the 5-percentile value from the two-parameter Weibull distribution. The 5-percentile value from the maximum

Table 5. Ratio of 5-Percentile Value to Mean Value.

Material Property (1)	Ratio of 5-percentile value to mean value		
	Two-parameter Weibull (2)	Three-parameter Weibull	
		Modified Moment Method (3)	Maximum Likelihood Method (4)
Longitudinal Tensile Strength			
VG 1-6	0.825	0.904	0.909
VG 7-12	0.754	0.817	0.814
VG 13-18	0.800	0.857	0.863
VG 19-24	0.817	0.876	0.888
PG	0.863	0.879	0.886
Longitudinal Compressive Strength			
VG 1-6			
VG 7-12	0.821	0.906	0.908
VG 13-18	0.805	0.839	0.853
VG 19-24	0.772	0.852	0.857
PG	0.785	0.847	0.847
PG-M	0.765	0.822	0.825
	0.811	0.834	0.841
Shear Strength			
VG 19-24	0.876	0.867	0.876
PG	0.802	0.862	0.874
Transverse Compressive Strength			
PG-M	0.857	0.910	0.913
Longitudinal Tensile Modulus			
VG 1-6	0.857	0.894	0.895
VG 7-12	0.857	0.824	0.857
VG 13-18	0.785	0.825	0.838
VG 19-24	0.899	0.931	0.934
PG	0.871	0.900	0.903
Longitudinal Compressive Modulus			
VG 1-6			
VG 7-12	0.884	0.912	0.918
VG 13-18	0.856	0.854	0.856
VG 19-24	0.748	0.814	0.826
PG	0.926	0.927	0.926
	0.914	0.932	0.936
Shear Modulus			
VG 19-24	0.760	0.815	0.760
PG	0.784	0.837	0.855

likelihood method parameters was just slightly greater than that obtained from the modified moment method parameters, about half a percent. Using the two-parameter Weibull distribution would result in lower estimates of the 5-percentile value relative to the three-parameter Weibull distribution. This is consistent with the results of Tenn (1981) who found that the two-parameter Weibull distribution resulted in lower allowable design values than the three-parameter Weibull, although he found only about a 1% decrease.

4.6 EFFECT OF DISTRIBUTION ON ALLOWABLE LOAD

A performance function is considered as follows.

$$g = R - L - D \tag{4.15}$$

where R is the resistance, L is a live load, D is a dead load, and g<0 is failure. The load is considered to be half dead load and half live load. The dead load is assumed to follow a normal distribution with a coefficient of variation of 0.10, and the live load is assumed to follow an Extreme Type I distribution with a coefficient of variation of 0.25. These are approximately the statistics and load ratio applicable to both building and bridge loads (Galambos et al., 1982, Nowak, 1995).

Each data set was used for the resistance, R, and a dead and live load, D and L, were determined using first-order reliability methods (Ang and Tang, 1984) such that the reliability index would be 3.00. Both the three-parameter Weibull distribution determined using the modified moment method and the maximum likelihood method were used. The ratios of the allowable load from the three-parameter Weibull distribution to the allowable load from the two-

parameter Weibull distribution are shown in Table 6.

The three-parameter Weibull distributions resulted in allowable loads that averaged 7% greater than allowable loads from the two-parameter Weibull distribution, with the modified moment method giving on the average just slightly higher allowable loads. Given the fact that different chosen probability distributions can result in allowable loads that vary by as much as 50% (Gromala et al, 1990), the 7% variation in allowable load is not very significant.

The allowable load was also examined for a live load to dead load ratio of four instead of one, a ratio based on composite structures being lighter, resulting in higher live to dead load ratios. For a live load to dead load ratio of 4, the allowable load from the three-parameter Weibull distributions averaged 3% greater than the allowable load using the two-parameter Weibull distribution. The decrease in the ratio of allowable loads was expected since the resistance statistics become less important as the uncertainty in the load increases with increasing live to dead load ratios. The 3% difference is virtually insignificant.

4.7 EVALUATION OF RESULTS

Not much difference was observed between the modified moment method and the maximum likelihood method for the three-parameter Weibull distribution. Both resulted in similar observed significance levels (OSL), nominal design values, and allowable loads. If a three-parameter Weibull distribution is to be used to characterize the data, it is recommended that the modified moment method be used. This is because of the relative ease in estimating the distribution parameters, the less likelihood in obtaining a negative location parameter, and the

Table 6. Ratio of Allowable Load from Three-Parameter Weibull to Two-Parameter Weibull for a Reliability Index of 3.00.

Material Property (1)	Ratio of allowable load to allowable load for two parameter Weibull distribution	
	Modified Moment Method (2)	Maximum Likelihood Method (3)
Longitudinal Tensile Strength		
VG 1-6	1.07	1.07
VG 7-12	1.18	1.18
VG 13-18	1.09	1.09
VG 19-24	1.08	1.08
PG	1.01	1.01
Longitudinal Compressive Strength		
VG 1-6		
VG 7-12	1.08	1.07
VG 13-18	1.07	1.08
VG 19-24	1.15	1.15
PG	1.12	1.12
PG-M	1.16	1.16
	1.05	1.06
Shear Strength		
VG 19-24	0.99	1.00
PG	1.09	1.09
Transverse Compressive Strength		
PG-M	1.03	1.03
Longitudinal Tensile Modulus		
VG 1-6	1.02	1.02
VG 7-12	0.95	1.00
VG 13-18	1.10	1.11
VG 19-24	1.00	1.00
PG	1.01	1.01
Longitudinal Compressive Modulus		
VG 1-6		
VG 7-12	1.00	1.00
VG 13-18	0.99	1.00
VG 19-24	1.20	1.21
PG	1.00	1.00
	1.00	1.00
Shear Modulus		
VG 19-24	1.16	1.00
PG	1.12	1.13

similarity in the results to those obtained using the maximum likelihood method.

The two-parameter Weibull distribution could not be rejected at the 5% level for 19 out of the 26 data sets. Although the two-parameter Weibull resulted in lower nominal design values and lower allowable loads than either of the three-parameter Weibull distributions, the differences were well less than ten percent. This difference is insignificant in most structural engineering applications.

Even though the three-parameter Weibull distribution is more robust than the two-parameter Weibull distribution, there are some problems with the three-parameter Weibull distribution. The basic conceptual problem is that there is a nonzero lower bound, which implies that for loads less than the lower bound there is no chance of failure. Average values of the lower bound, or location parameter, were within 10% of the first order statistic, and were about 80% of the mean value. If additional data were to be collected such that, for example, the sample size was doubled, the scale parameter would undoubtedly decrease.

4.8 CONCLUSIONS

The three-parameter and two-parameter Weibull distributions were compared using 26 sets of data on fiber-reinforced polymeric pultruded composite material mechanical properties. Both strength and stiffness properties were examined. It is recommended that the two-parameter Weibull distribution be used to characterize FRP composite material properties. The primary bases for this recommendation are small differences in nominal design values and small differences in allowable loads between the two-parameter and three-parameter Weibull distributions. Other supporting reasons for the recommendation are

similar observed significance levels in distribution fitting, computational efficiency, and the fact that the location parameter of the three-parameter Weibull distribution is near the first order statistic. The last reason implies that there is a load near the lowest data point that can be applied to the structural member for which there is no chance of failure. This seems counterintuitive, as it seems reasonable that there would be some chance of failure at any load level, albeit the probability could be quite small.

CHAPTER 5

DEVELOPMENT OF RESISTANCE FACTORS

5.1 TARGET RELIABILITY INDEX (β)

Probabilistic design is based on achieving a certain reliability level, often expressed as a target reliability index, β. For most materials the target reliability index can be obtained by examining current design practice. This process is often referred to as code calibration and makes use of the many years of successful design practice. With FRP materials, there is not this design experience, and thus typical code calibration cannot be used. Rather a target reliability index has to be chosen that would represent an adequate safety level.

The target reliability index should depend on the mode and the consequences of approaching various limit states. Ellingwood (2000) suggested a reliability index of 2.5 for a ductile failure mode and not serious consequence of failure, 3.0 for either a ductile failure mode and serious consequence or a brittle failure mode and not serious failure consequence, and 4.0 for a brittle failure mode and serious consequence. Ellingwood (2000) suggested that the target reliability index be set to approximately 3.5 for FRP materials, because they exhibit little ductility.

The reliability index for hot-rolled steel, cold-formed steel, reinforced or prestressed concrete, and engineered wood elements designed by LRFD specifications tend to fall in the range of 2.2 to 3.0 (Ellingwood, 2000). Specifically for short tied reinforced concrete columns failing through concrete

crushing, or the failure being above the balanced point, the reliability index is approximately 3.2 (Ellingwood et al, 1980). For short tied columns failing through steel yielding, or failure being below the balanced point, the reliability index is approximately 4.1 when the resistance factor is 0.9 and 3.0 when the resistance factor is 0.7. For short spiral columns failing through concrete compression, the reliability index is approximately 2.9. Israel et al (1987) report a reliability index of approximately 2.7 for concentrically loaded short reinforced concrete columns with 1% reinforcing and 3.5 for columns with 3% reinforcing. For concentrically loaded steel columns, Ellingwood et al. (1980) reported the reliability index as a function of the slenderness ratio λ, which is defined as the square root of the yield stress divided by the Euler buckling stress. For λ=0.3 (short column) the reliability index is approximately 3.3. The reliability index decreases to approximately 2.3 for λ in the range of 1.1-1.3, and then increases back to 3.2 for λ=1.9 (long column).

The target reliability index chosen for the development of the engineered wood construction LRFD standard (AF&PA/ASCE 16-95) was 2.4. Ellingwood (1997) gives the background for this selection. Glulam beams designed by allowable stress design (ASD) and subjected to occupancy live loads had a reliability index in the range of 2.6 to 2.7. Roof beams designed for snow loads had reliability indices in the range of 2.1 to 2.2. The target reliability index of 2.4 was approximately an average of the reliability inherent in ASD design of beams subjected to occupancy and snow loads.

Hsiao et al. (1990) suggest a very similar target reliability index, 2.5 for members, for the development of LRFD criteria for cold-formed steel. Ellingwood (1997) reported a reliability index of 2.4 for cold-formed steel tension members and concentrically loaded compression members, 2.7 for flexure in laterally supported beams, and 2.5 for lateral-torsional buckling. These values are similar to the reliability in hot-rolled steel. The American Institute of Steel Construction LRFD spec (AISC, 1993) reports an implied beta of approximately 2.6 for members.

Gromala et al. (1990) point out that the reliability index is a function of the chosen probability distributions. For a set of wood member data, they obtained a reliability index of 2.9 when using a Weibull distribution for the resistance and a reliability index of 3.6 when using a lognormal distribution for the resistance.

For this study, a target reliability of 3.0 for buckling and local failures (long columns), 3.5 for material failures (short columns) and 3.0 for lateral-torsional buckling failures (beams) was chosen. These target reliability indices for FRP members are slightly higher than those used in the development of the wood and cold-formed steel specifications. The reasoning is that a higher reliability index is justified for a material with which we have little design experience. FRP materials tend to be more brittle than other types of materials, which would also justify a higher reliability index. For FRP members under axial compression, material failures are more brittle than buckling failures, which justifies using a higher reliability index for material failures. The target reliability

indices are appropriate for gravity loadings (dead and live load) and will be used to develop resistance factors.

5.2 PROBABILISTIC BASED DESIGN

The coefficient of variation of material properties for well-established materials like steel and concrete has been taken as a constant due to the stability and uniformity of the production process. For FRP materials, the coefficient of variation of material properties will be a function of such things as fiber type, fiber volume, lay-up, and quality control procedures. The manufacturer has some control over the coefficient of variation. Thus, the resistance factor will be developed as a function of the coefficient of variation. Coefficients of variation for material properties (modulus of elasticity, compressive strength) of 0.05, 0.075, 0.10, 0.15, 0.20, 0.25 were considered in this study. This range of coefficients of variations was considered because it bounds the uncertainty expected in FRP materials.

The FRP material properties were considered to follow a two-parameter Weibull distribution. The Weibull distribution has been the most common probability distribution to be used with FRP material properties (King, 1986, Rust et al., 1989). The dead load was assumed to follow a normal distribution with a mean of 1.05 times the nominal value, D_n, and a CV of 0.10 (Galambos et al., 1982). The live load was assumed to follow an Extreme Type I distribution with a mean value equal to the nominal value, L_n, and a CV of 0.25 (Galambos et al., 1982). Nominal live load to dead load ratios of 0.5, 1.0, 2.0, 3.0, 4.0 were considered. Cross sectional properties and the unbraced length were considered

to be deterministic. The resistance factor was found based on the equation,

$$1.2D_n + 1.6L_n = \varphi R_n \tag{5.1}$$

where R_n is the nominal resistance calculated using nominal (5-percentile) material properties and ϕ is the resistance factor.

The performance function used for this analysis is as follows:

$$g = XR - D - L \tag{5.2}$$

where g is the performance function such that $g < 0$ failure, $g = 0$ is the limit state, and $g>0$ is safe, R is the resistance, D is the dead load, L is the live load, and X is a model error. The model error is a random variable that accounts for both systematic and random errors in the prediction of the resistance. It is obtained from the statistics of the ratio of experimentally obtained resistances to the predicted resistances.

First-order reliability methods (Ang and Tang, 1994) are used to find a resistance from equation 5.2 such that the target reliability index is met. The corresponding nominal resistance is obtained, and equation 5.1 is used to determine the necessary resistance factor to obtain this nominal resistance.

5.3 DOUBLY SYMMETRIC CROSS-SECTIONS

Zureick and Scott (1997) tested four different doubly symmetric cross-sections, two wide flange sections and two box sections subjected to concentric axial compression. The specimens were made using a vinylester matrix and E-glass rovings and nonwoven mats. Six specimens of each cross section were tested, resulting in 24 total specimens. Twenty-two of these specimens failed in

global buckling and will be used in this analysis. The slenderness ratios varied from 36 to 103. Zureick and Scott (1997) proposed two analytical formulas for the buckling load of axially loaded polymer columns. The first is similar to Euler's buckling load.

$$P_E = \frac{\pi^2 E_L}{\left(\frac{KL}{r}\right)^2_{\min}} A_g \tag{5.3}$$

where P_E is the buckling load, E_L is the longitudinal elastic compressive modulus, r is the radius of gyration, KL is the effective unbraced length, and A_g is the gross area. The ratio of the experimental buckling load, P_{exp}, to P_E ranged from 0.85 to 0.97 with an average of 0.92 and a standard deviation of 0.038.

The second proposed analytical formula was a modification to equation 5.3 that accounts for shear deformations.

$$P_e = \frac{P_E}{1 + (n_s \ P_E / \ A_g \ G_{LT})} \tag{5.4}$$

where n_s is the shear factor for the specific cross section and G_{LT} is the in-plane shear modulus. The ratio of P_{exp}/P_e ranged from 0.88 to 1.01 with an average of 0.94 and a standard deviation of 0.039. Equation 5.4 was slightly more accurate than equation 5.3, but both equations had about the same amount of precision. The ratio of the experimental resistance to the calculated resistance, or the model error, was fit by a normal distribution.

The difference in prediction of buckling strength between equations 5.3 and 5.4 will be a function of the ratio of E_L/G_{LT}. For the columns tested by

Zurieck and Scott (1997), the ratio of E_L/G_{LT} ranged from 3.8 to 6.8 with an average of 5.1. They recommend that equation 5.3 is adequate for ratios of E_L/G_{LT} less than 6 for short-term behavior. For long-term behavior, Zurieck and Scott (1997) recommend the use of equation 5.4. Their reasoning is that the in-plane shear modulus G_{LT} is much more matrix-dependent than the longitudinal elastic modulus and will therefore be more susceptible to degradation over time.

The resistance factors developed using equation 5.3 are included in table 7. Figure 3 shows the resistance factor obtained using equation 5.3 for the resistance vs. the nominal live load to dead load ratio, L_n/D_n, for different coefficients of variation of the longitudinal modulus, $(CV)_{E_L}$.

The resistance factor is almost constant with varying L_n/D_n ratios, and generally decreases with increasing $(CV)_{E_L}$. An interesting phenomenon occurs for small coefficients of variation of E_L; the resistance factor actually decreases with decreasing $(CV)_{E_L}$. This can be explained by looking at Figure 4 that shows three relationships for the case of L_n/D_n=4.0. One line shows a resistance factor based on using the mean value of E_L instead of the nominal value. The resistance factor increases with decreasing $(CV)_{E_L}$. A second line shows the ratio of the mean value of E_L to the nominal, or fifth percentile, value of E_L. The resistance factor for use with the nominal value of E is found by multiplying the resistance factor based on mean of E_L by the ratio of mean to nominal. Since the ratio of the mean to the nominal is decreasing faster than the resistance factor based on the mean value is increasing, the resistance factor based on nominal values does

Table 7. Resistance Factors for Doubly Symmetric Columns with Buckling Failure Using Equation 5.3.

Resistance Factor (ϕ)					
	Ln/Dn				
COV	**0.5**	**1.0**	**2.0**	**3.0**	**4.0**
0.050	0.887	0.850	0.808	0.787	0.776
0.075	0.873	0.862	0.827	0.810	0.800
0.100	0.832	0.843	0.828	0.816	0.808
0.150	0.727	0.755	0.766	0.768	0.767
0.200	0.622	0.652	0.673	0.679	0.683
0.250	0.526	0.554	0.576	0.585	0.590

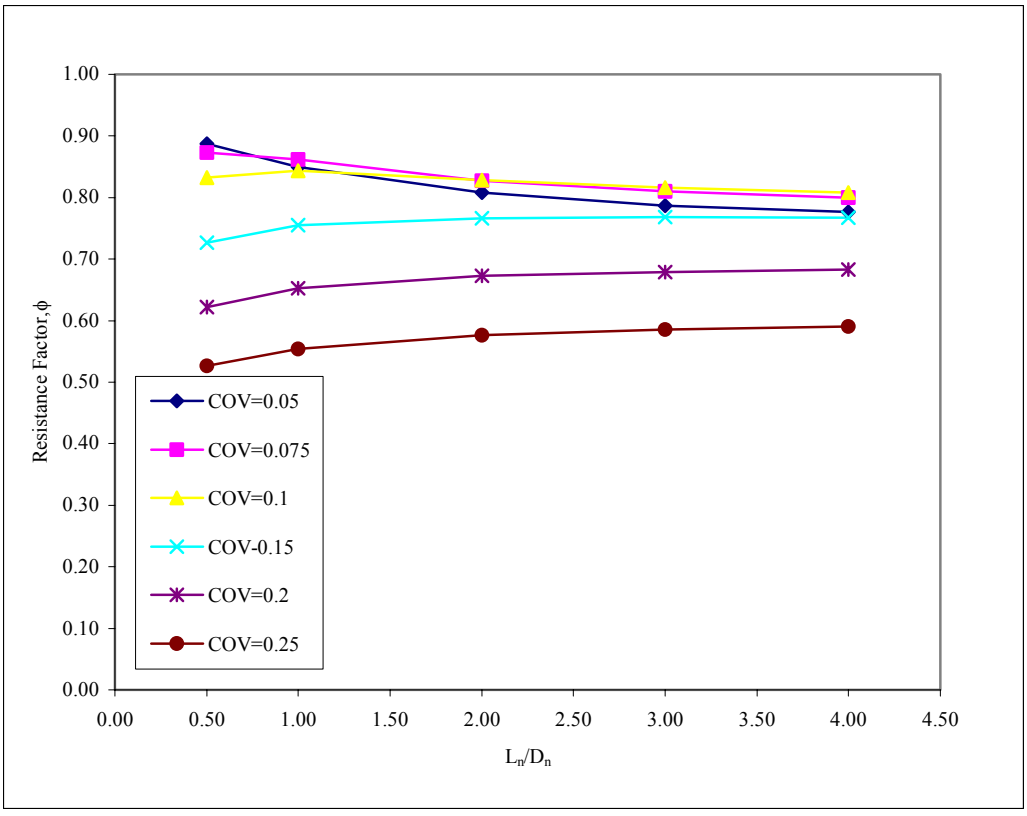

Figure 3. Resistance Factors vs. L_n/D_n for Buckling Failure of Doubly Symmetric Columns.

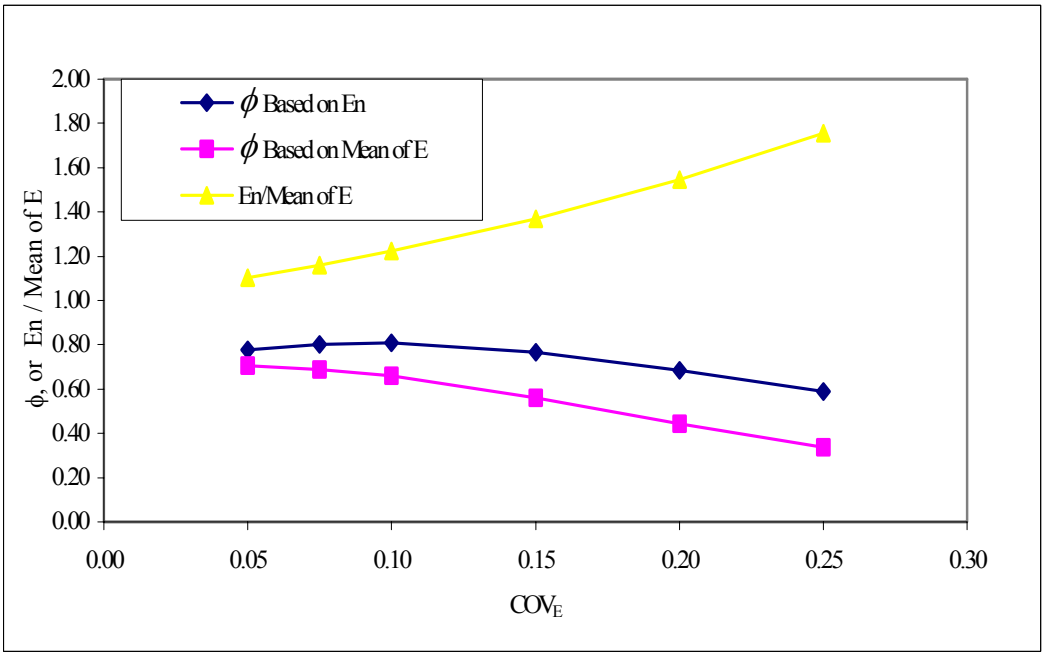

Figure 4. $L_n/D_n = 4.0$

actually decrease with decreasing $(CV)_{E_L}$ at some point.

The resistance factor versus the coefficient of variation of E_L is plotted in Figure 5 for all L_n/D_n ratios. A reasonable fit to the data is a constant resistance factor for $(CV)_{E_L} \le 0.1$, and a resistance factor that is a linear function of the coefficient of variation for $(CV)_{E_L} > 0.1$. The resistance factor using best-fit lines for the data would be:

$$\phi = 1.00 - 1.75(CV_{E_L}) \le 0.83 \qquad (5.5)$$

Thus, it is proposed that rather than a constant resistance factor, the resistance factor be a function of $(CV)_{E_L}$, or the uncertainty level in the FRP material property. The resistance factor would increase with a decreasing coefficient of variation of the longitudinal compressive modulus. A constant value of $\phi = 0.83$

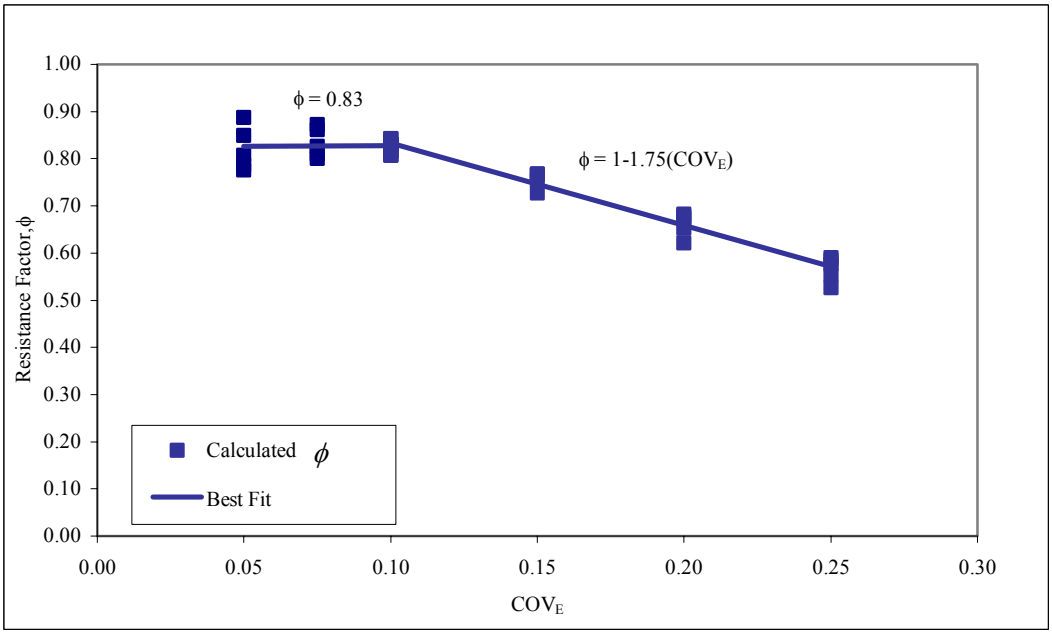

Figure 5. Resistance Factors for Doubly Symmetric Cross-Sections with Buckling Failure Based on E_n for all L_n/D_n Using Model Error of Equation 5.3.

is suggested for $(CV)_{E_L} \le 0.10$ which might suggest that there is no benefit to the manufacturer for reducing the $(CV)_{E_L}$ when it is less than 0.10. This is not true, as a smaller $(CV)_{E_L}$ would result in a larger nominal value for a given mean value.

The resistance factors, assuming E_L and G_{LT} perfectly correlated, developed using equation 5.4 are shown in table 8. The determination of the resistance factor for equation 5.4 that includes shear deformations would require knowledge of the joint probability distribution of E_L and G_{LT}. Even first-order information, the correlation coefficient between E_L and G_{LT}, is not known. However, bounds can be established by first assuming E_L and G_{LT} to be

Table 8. Resistance Factors for Doubly Symmetric Columns with Buckling Failure Using Equation 5.4 (E_L and G_{LT} perfectly correlated).

Resistance Factor (ϕ)					
	Ln/Dn				
COV	**0.5**	**1.0**	**2.0**	**3.0**	**4.0**
0.050	0.906	0.868	0.825	0.804	0.794
0.075	0.892	0.880	0.845	0.827	0.817
0.100	0.849	0.861	0.846	0.834	0.826
0.150	0.743	0.770	0.783	0.785	0.783
0.200	0.636	0.666	0.687	0.695	0.697
0.250	0.536	0.565	0.587	0.559	0.602

statistically independent, and then assuming E_L and G_{LT} to be perfectly correlated. Results for these two assumptions are shown in Table 9 for different values of the slenderness ratio L/r, the nominal live load to dead load ratio L_n/D_n, and the ratio of the mean values, $\mu_{E_L} / \mu_{G_{LT}}$. The ratio of $\mu_{E_L} / \mu_{G_{LT}} = 6$ is typical of glass fibers and the ratio $\mu_{E_L} / \mu_{G_{LT}} = 20$ is typical of carbon fibers. It is assumed in Table 9 that both E_L and G_{LT} have the same coefficient of variation.

It is seen in Table 9 that there is little difference between the resistance factor for assuming statistical independence and assuming perfect correlation. The resistance factors for assuming perfect correlation average 3.4% less than for assuming statistical independence. Also given in Table 9 are the resistance factors from equation 5.5. It is seen that equation 5.5 tends to be slightly conservative, with the resistance factor averaging 3.3% less than that for assuming perfect correlation between E_L and G_{LT}. For simplicity, it is

Table 9. Resistance Factors for Different Assumptions Concerning E_L and G_{LT}.

CV	L_n/D_n	L/r	$\mu_{E_L} / \mu_{G_{LT}}$	Resistance Factors		
				E_L and G_{LT} Independent	E_L and G_{LT} Perfectly Correlated	Equation 5.5
0.1	1	40	6	0.879	0.861	0.825
			20	0.909		
		100	6	0.864		
			20	0.871		
	4	40	6	0.836	0.825	
			20	0.853		
		100	6	0.827		
			20	0.831		
0.2	1	40	6	0.696	0.666	0.650
			20	0.763		
		100	6	0.671		
			20	0.683		
	4	40	6	0.728	0.697	
			20	0.791		
		100	6	0.702		
			20	0.714		

recommended that equation 5.5 be used to determine the resistance factor for buckling of doubly symmetric cross-sections whether equation 5.3 or equation 5.4 is used to determine the buckling load. Equation 5.4 should be used to determine the buckling load when the material properties are such that shear deformations are significant.

5.4 LOCAL BUCKLING FOR DOUBLY SYMMETRIC CROSS-SECTIONS

Yoon (1993) investigated experimentally and analytically short-term compression behavior for axially loaded I-shaped FRP columns. He tested a total of thirty-two I-shaped columns made from pultruded fiber reinforced polymer materials. Twenty-two specimens were made using a polyester matrix, and ten specimens were made using a vinylester matrix. The sizes and lengths for these specimens were selected so that local buckling occurred at loads less than those which would cause global buckling or material failure. The lengths varied from 35 in. to 120 in., with slenderness ratios ranging from 20 to 50. The width to thickness ratios of the flange ranged from 6 to 13 and the depth to thickness ratios for the web ranged from 15 to 26. The experiment was terminated at the post buckling stage. After applying the load, the column specimen was observed until the out-of-plane deflections at the tips of the flange occurred. Critical buckling loads were experimentally determined and compared to the analytical critical buckling loads.

An analytical solution was developed for the prediction of the local buckling loads for pultruded columns composed of flat plates under short-term

axial loads. The proposed solution is based on the classical orthotropic plate theory. It accounts for the rotational restraint at the junction of the web and the flange.

$$\sigma_{cr} = \frac{\pi^2 \sqrt{E_{11} E_{22}}}{12\,(1 - \nu_{12}\nu_{21})(b/t)^2} \tag{5.6}$$

where,

σ_{cr} : the critical buckling stress.

E_{11} : major Young's modulus.

E_{22} :minor Young's modulus.

ν_{12} : major Poisson's ratio, $|\nu_{12}| < \sqrt{\frac{E_{11}}{E_{22}}}$.

ν_{21} : minor Poisson's ratio, $|\nu_{21}| < \sqrt{\frac{E_{22}}{E_{11}}}$.

t: the thickness of the plate.

b: the width of the plate or half the with of the flange.

Tension and compression tests were performed to estimate the material properties E_{11}, E_{22}, ν_{12}, and ν_{21}. The average values for E_{11} and E_{22} in tension and compression tests were almost identical. The experimental local buckling loads ($P_{\exp}$) were compared to those predicted theoretically (P_{pred}) using equations 5.6. The major Poisson's ratio (ν_{12}) and the minor Poisson's ratio (ν_{21}) are considered to be constants since changing ν_{12} and ν_{21} by up to 50% has a small effect on the critical buckling stress (<3%). The major Young's modulus of

elasticity (E_{11}) and the minor Young's modulus of elasticity (E_{22}) are considered to be the random variables. Data values (thirty-two specimens) for both variables developed by Yoon (1993) were used to determine the correlation between them. The correlation coefficient between E_{11} and E_{22} was calculated to be 0.353. The correlation coefficient (0.353) was compared to the value from equation 3.16 (Sachs, 1983) for two sided test at 5% level with degrees of freedom equal to the number of data point minus two (DF=n-2). For n=32, the corresponding value is 0.349. Since the correlation coefficient (0.353) is very close to the corresponding value using equation 3.16 (more by 1%), both E_{11} and E_{22} are considered to be independent random variables. Both random variables are assumed to fit the two-parameter Weibull Distribution.

Experimental results for local buckling tests were compared to the analytical results. The ratio of the experimental critical load, $P_{\exp}$, to the analytical critical load, P_{anal}, ranged from 0.844 to 1.42 with an average of 1.07 and a standard deviation of 0.146 (Yoon, 1993). The ratio of the experimental resistance to the calculated resistance, or the model error, was fit by a normal distribution. The resistance factors were developed using equation 5.6 for all cases of L_n/D_n (0.5, 1.0, 2.0, 3.0, and 4.0). The resistance factor is almost constant with varying L_n/D_n. The average values of the resistance factors are considered in this analysis. All values for the resistance factors are tabulated in table 10. Based on data developed by Yoon (1993), μ_{E11}/μ_{E22} is assumed to be

Table 10. Resistance Factors for Columns with Local Bucking Using Equation 5.6.

Resistance Factor (ϕ), L_n/D_n = 0.5							Resistance Factor (ϕ), L_n/D_n = 1						
	COV_E							COV_E					
COV_G	0.05	0.075	0.1	0.15	0.2	0.25	COV_G	0.05	0.075	0.1	0.15	0.2	0.25
0.050	0.854	0.871	0.888	0.910	0.901	0.865	**0.050**	0.857	0.876	0.894	0.925	0.921	0.891
0.075	0.871	0.891	0.909	0.931	0.922	0.885	**0.075**	0.876	0.895	0.914	0.946	0.942	0.914
0.100	0.895	0.907	0.927	0.948	0.943	0.905	**0.100**	0.894	0.914	0.933	0.965	0.962	0.936
0.150	0.91	0.931	0.948	0.974	0.975	0.942	**0.150**	0.92	0.940	0.960	0.990	0.999	0.975
0.200	0.901	0.922	0.943	0.975	0.988	0.970	**0.200**	0.921	0.942	0.962	0.997	1.015	1.002
0.250	0.865	0.885	0.905	0.942	0.968	0.974	**0.250**	0.891	0.913	0.935	0.975	1.002	1.011
Resistance Factor (ϕ), L_n/D_n = 2							**Resistance Factor (ϕ), L_n/D_n = 3**						
	COV_E							COV_E					
COV_G	0.05	0.075	0.1	0.15	0.2	0.25	COV_G	0.05	0.075	0.1	0.15	0.2	0.25
0.050	0.836	0.857	0.872	0.903	0.914	0.899	**0.050**	0.824	0.843	0.860	0.892	0.908	0.899
0.075	0.857	0.875	0.895	0.923	0.937	0.922	**0.075**	0.843	0.861	0.881	0.911	0.930	0.921
0.100	0.873	0.893	0.912	0.945	0.957	0.944	**0.100**	0.860	0.881	0.900	0.931	0.951	0.940
0.150	0.903	0.923	0.945	0.977	0.995	0.983	**0.150**	0.892	0.911	0.931	0.965	0.987	0.981
0.200	0.914	0.937	0.957	0.995	1.051	1.014	**0.200**	0.906	0.930	0.951	0.987	1.009	1.014
0.250	0.899	0.922	0.942	0.983	1.013	1.024	**0.250**	0.899	0.919	0.940	0.979	1.014	1.028
Resistance Factor (ϕ), L_n/D_n = 4							**Resistance Factor (ϕ), L_n/D_n Average**						
	COV_E							COV_E					
COV_G	0.05	0.075	0.1	0.15	0.2	0.25	COV_G	0.05	0.075	0.1	0.15	0.2	0.25
0.050	0.816	0.833	0.852	0.884	0.902	0.894	**0.050**	0.837	0.856	0.873	0.903	0.909	0.890
0.075	0.832	0.854	0.873	0.904	0.923	0.917	**0.075**	0.856	0.875	0.894	0.923	0.931	0.912
0.100	0.853	0.871	0.891	0.925	0.944	0.940	**0.100**	0.875	0.893	0.913	0.943	0.951	0.933
0.150	0.882	0.903	0.925	0.960	0.979	0.978	**0.150**	0.901	0.922	0.942	0.973	0.987	0.972
0.200	0.902	0.923	0.944	0.979	1.006	1.013	**0.200**	0.909	0.931	0.951	0.987	1.014	1.003
0.250	0.897	0.918	0.939	0.978	1.012	1.025	**0.250**	0.890	0.911	0.932	0.971	1.002	1.012

1.8. Changing the ratio μ_{E11}/μ_{E22} has no effect on the resistance factors. Figure 6 shows the resistance factors obtained from equation 5.6 for resistance vs. COV for both E_{11} and E_{22}. Figure 6 shows that the resistance factor is almost constant regardless of the coefficient of variation of E_{11} and E_{22} for all values of coefficient of variations. The resistance factor using the best-fit surface for the data would be:

$$\phi = 0.93 \qquad \text{for all values of } (CV)_{E11} \text{ and } (CV)_{E22} \tag{5.7}$$

An interesting phenomenon occurs for the case when $(CV)_{E11}$ and $(CV)_{E22}$ are equal; the resistance factor actually decreases with decreasing $(CV)_E$. This can be explained by looking at Figure 7 that shows three relationships for the case of L_n/D_n=1.0. One line shows a resistance factor based on using the mean value of E instead of the nominal value. The resistance factor increases with decreasing $(CV)_E$. A second line shows the ratio of the mean value of E to the nominal, or fifth percentile, value of E. The resistance factor for use with the nominal value of E is found by multiplying the resistance factor based on mean of E by the ratio of mean to nominal. Since the ratio of the mean to the nominal is decreasing faster than the resistance factor based on the mean value is increasing, the resistance factor based on nominal values does actually decrease with decreasing $(CV)_E$ when $(CV)_{E11} = (CV)_{E22}$.

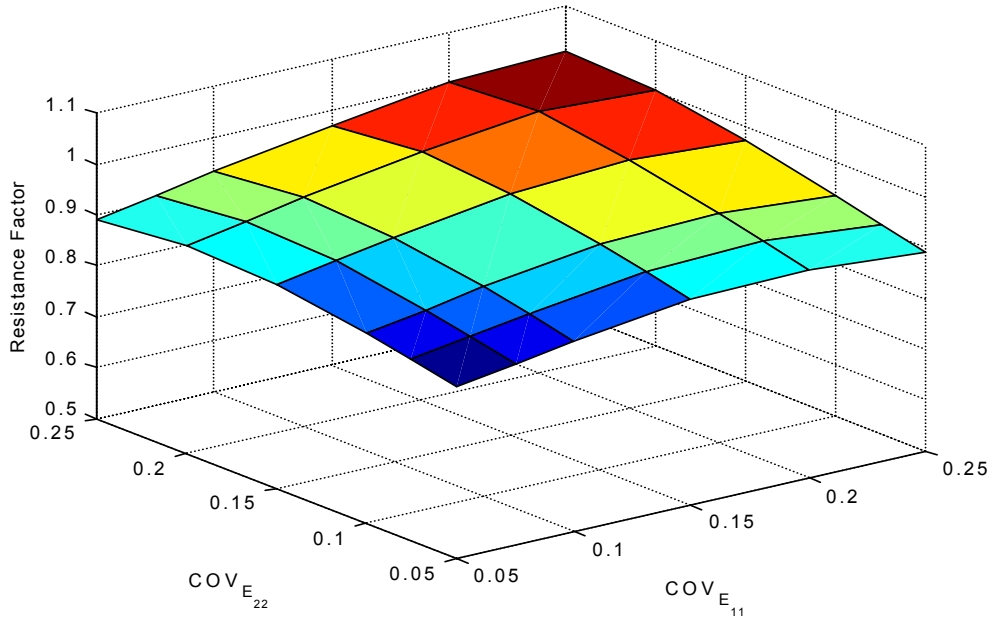

Figure 6. Resistance Factors for Doubly Symmetric Cross-Sections with Local Buckling Failure vs. COV of E_{11} and E_{22}.

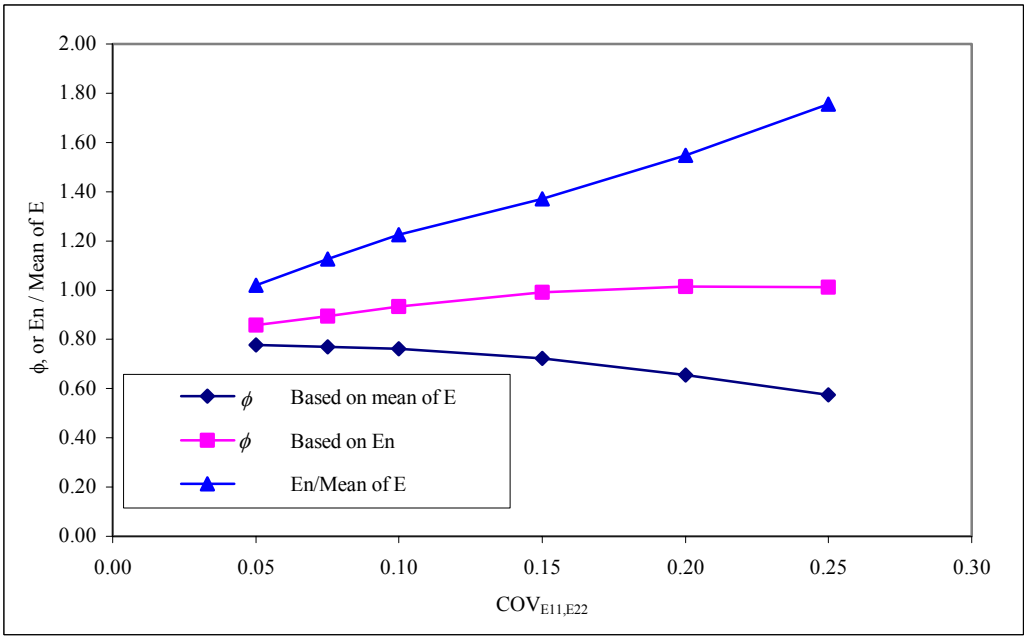

Figure 7. $L_n / D_n = 1.0$

5.5 EQUAL LEG ANGLE CROSS – SECTIONS

Zureick and Steffen (2000) tested 25 concentrically loaded equal-leg single angle FRP members with slenderness ratios from 30 to 105. All specimens had E-glass reinforcement, with seven having a polyester matrix and eighteen having a vinylester matrix. Buckling occurred in either a flexural mode (flexure about the minor principal axis) or a flexural-torsional mode (flexure about the major principal axis and twist about the member longitudinal axis). For the flexural mode, the critical buckling load is of the form (Zureick and Steffen, 2000):

$$P_{ez} = \frac{\pi^2 E_L}{\left(\frac{KL_z}{r_z}\right)^2} A_g \tag{5.8}$$

where P_{ez} is the flexural buckling load about the minor principal axis, or the z-axis. Seven specimens failed in this mode. The ratio of P_{exp}/P_{ez} ranged from 0.74 to 0.93 with an average of 0.81 and a standard deviation of 0.065. A lognormal distribution provided an adequate fit to the model error. The resistance factors determined using equation 5.8 are shown in table 11. Figure 8 shows the resistance factor obtained using equation 5.8 for the resistance vs. the coefficients of variation of the longitudinal modulus, $(CV)_{E_L}$ for all L_n / D_n ratios. Based on best fit lines, a resistance factor for the limit state of flexural buckling would be:

$$\phi = 0.84 - 1.35\left(CV_{E_L}\right) \leq 0.71 \tag{5.9}$$

For the flexural-torsional mode, the critical buckling load can be shown to have the form (Zureick and Steffen, 2000):

Table 11. Resistance Factors for Equal Leg Columns with Flexural Bucking Using Equation 5.8.

Resistance Factor (ϕ)					
	Ln/Dn				
COV	**0.5**	**1.0**	**2.0**	**3.0**	**4.0**
0.050	0.747	0.721	0.689	0.673	0.664
0.075	0.741	0.733	0.708	0.693	0.685
0.100	0.712	0.722	0.710	0.700	0.693
0.150	0.627	0.651	0.661	0.663	0.661
0.200	0.539	0.565	0.583	0.589	0.592
0.250	0.457	0.481	0.500	0.508	0.512

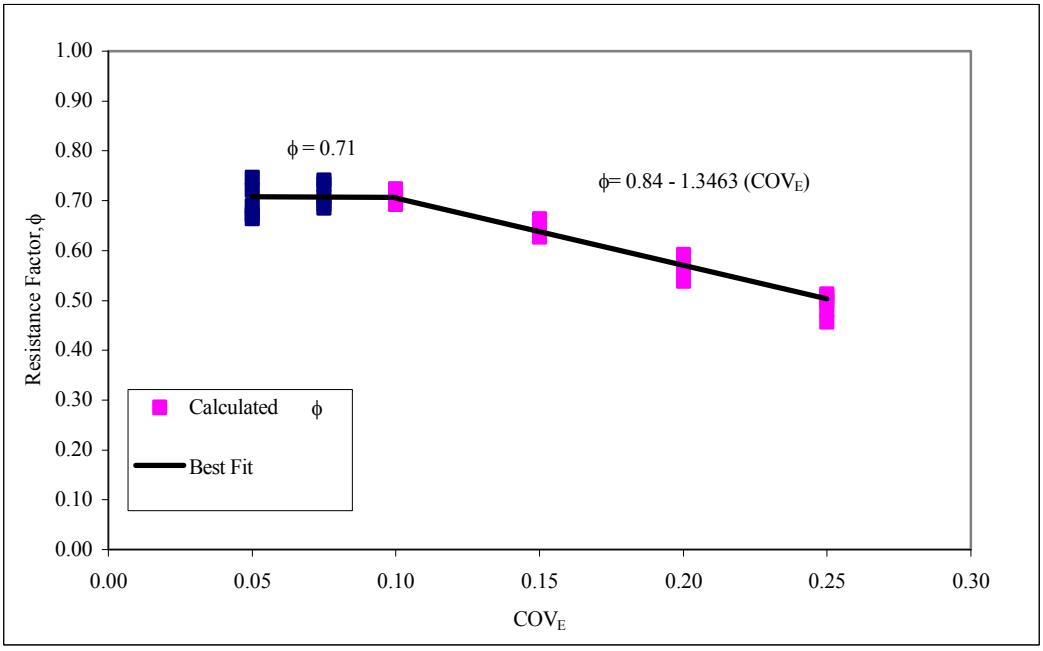

Figure 8. Resistance Factors for Equal Leg Single Angle-Sections with Flexural Buckling Failure Based on E_n for all L_n/D_n Using Model Error of Equation 5.8.

$$P_{ft} = \frac{P_{ey} + P_{ex}}{2H}\left[1 - \sqrt{1 - \frac{4H\,P_{ey}\,P_{ex}}{(P_{ey} + P_{ex})^2}}\right] \tag{5.10}$$

where P_{ft} is the flexural-torsional buckling load, P_{ey} is the buckling load about the major principal y-axis, P_{ex} is the torsional buckling load about the longitudinal x-axis, and H is combined material and geometrical constant with the details in Zureick and Steffen (2000). Eighteen specimens failed in this mode. The ratio of P_{exp}/P_{ft} ranged from 0.97 to 1.39 with an average of 1.14 and a standard deviation of 0.126. Besides the analytical difficulty of equation 5.10, the development of a resistance factor would require knowledge of the joint probability distribution of E_L, G_{LT}, and the major and minor Poisson's ratios, ν_{LT} and ν_{TL}.

Zureick and Steffen (2000) developed a simplification to Equation 5.10 for $E_L/G_{LT}<20$:

$$P_{ft} = 0.9\frac{G_{LT}}{\left(\frac{b}{t}\right)^2}A_g \tag{5.11}$$

where b is the width of a leg and t is the thickness of a leg. The ratio of P_{exp}/P_{ft} with P_{ft} obtained from equation 5.11 ranged from 1.08 to 1.66 with an average of 1.31 and a standard deviation of 0.135. A normal distribution provided an adequate fit for the model error.

Equation 5.11 over predicts the flexural-torsional buckling loads and results in resistance factors greater than 1.0 for coefficients of variation less than 0.135. This equation has been modified, by multiplying the flexural-torsional buckling loads by the mean of the model error, 1.31. The constant becomes 1.2,

which is the old constant, 0.9, times 1.31, resulting in Equation 5.12.

$$P_{ft} = 1.2 \frac{G_{LT}}{\left(\frac{b}{t}\right)^2} A_g \tag{5.12}$$

The modified model error has a mean of 1.0 and a CV of 0.17. The resistance factors developed using equation 5.12 are shown in table 12.

Figure 9 shows the resistance factor obtained using equation 5.12 for the resistance vs. the coefficients of variation of the longitudinal modulus, $(CV)_{E_L}$ for all L_n / D_n ratios. The resistance factor according to the best-fit lines for the data would be:

$$\phi = 0.93 - 0.87\left(CV_{G_{LT}}\right) \leq 0.84 \tag{5.13}$$

5.6 MATERIAL FAILURES (SHORT COLUMNS)

Short columns will fail by a material failure, or crushing. The resistance is determined as $P = (F_C)_L Ag$, where $(F_C)_L$ is the longitudinal compressive strength. No model error is necessary for material failure as $(F_C)_L$ was found as a load divided by an area, or using the same prediction equation. The resistance factors developed for material failure are included in table 13.

Figure 10 shows the resistance factor obtained for the resistance vs. the coefficients of variation of the longitudinal modulus, $(CV)_{E_L}$ for all L_n / D_n ratios. The resistance factor according to the best-fit line for the data would be:

$$\phi = 1.03 - 2.40\left(CV_{(F_C)_L}\right) \leq 0.79 \tag{5.14}$$

The CV of the longitudinal compressive strength, $(F_C)_L$, will be a function

Table 12. Resistance Factors for Equal Leg Columns with Flexural-Torsional Bucking Using Equation 5.12.

Resistance Factor (ϕ)					
	Ln/Dn				
COV	**0.5**	**1.0**	**2.0**	**3.0**	**4.0**
0.050	0.787	0.836	0.858	0.848	0.781
0.075	0.807	0.837	0.853	0.848	0.614
0.100	0.807	0.831	0.849	0.711	0.646
0.150	0.801	0.826	0.800	0.745	0.672
0.200	0.796	0.833	0.831	0.769	0.683
0.250	0.816	0.856	0.846	0.777	0.688

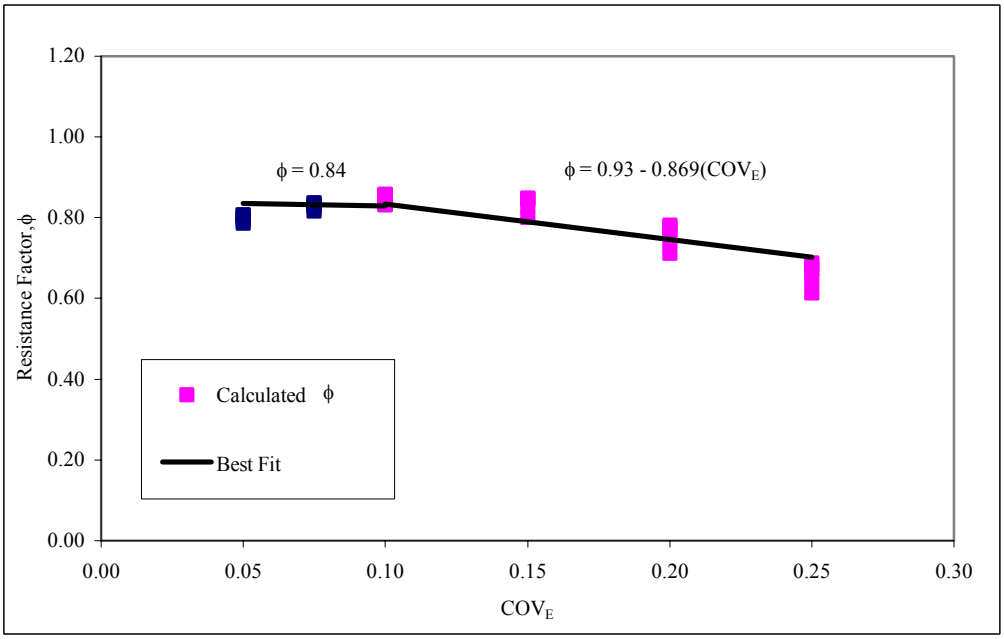

Figure 9. Resistance Factors for Equal Leg Single Angle-Sections with Flexural-Torsional Buckling Failure Based on E_n for all L_n/D_n Using Model Error of Equation 5.12.

Table 13 Resistance Factors for Material Failure.

Resistance Factor (ϕ)					
	Ln/Dn				
COV	**0.5**	**1.0**	**2.0**	**3.0**	**4.0**
0.050	0.818	0.645	0.463	0.324	0.222
0.075	0.742	0.724	0.685	0.667	0.655
0.100	0.764	0.651	0.481	0.339	0.234
0.150	0.712	0.635	0.488	0.350	0.242
0.200	0.688	0.623	0.488	0.353	0.247
0.250	0.675	0.615	0.487	0.355	0.249

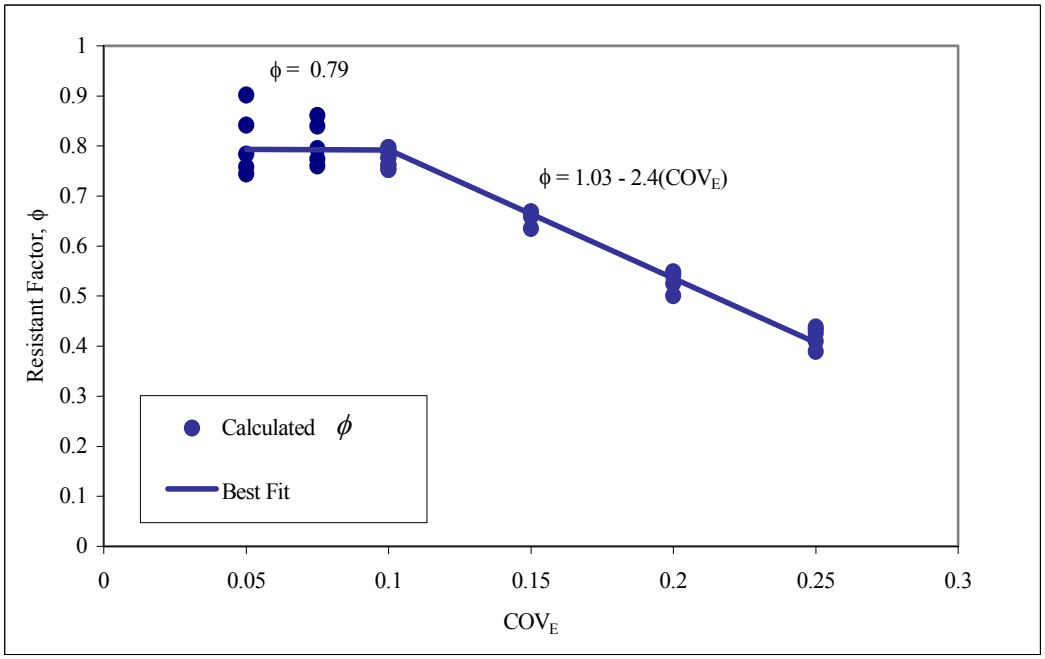

Figure 10. Resistance Factors for all Cross-Sections of Material Failure Based on E_n for all L_n/D_n.

of the specimen width. Coupon specimens with a greater width will have less variation than specimens with a smaller width. Typically a 25 mm wide specimen is tested. As most actual cross-sections will have widths greater than this, the actual CV of the strength of the cross-section will probably be less than the CV of the coupon. Using the CV of the coupon in equation 5.14 will thus typically be conservative.

5.7 DOUBLY SYMMETRIC SIMPLY SUPPORTED BEAMS

Stoddard (1997) investigated experimentally and analytically the lateral-torsional behavior of hybrid (E-glass and carbon fiber) and non-hybrid (all glass fiber) FRP I-shaped beams subjected to vertical concentrated short term loading acting at mid-spans. Five different I-shaped 4 x 2 x ¼ in. reinforced cross sections were tested. Eight specimens were used in this study. Elastic lateral-torsional buckling of doubly symmetric FRP beams was predicted theoretically using three approaches.

Three analytical approaches were presented to calculate the lateral-torsional buckling loads. The first approach is the classical one-dimensional isotropic theory derived by Timosheko and Gere (1961) for thin walled slender I-shaped loaded with pure moment around the X-axis. The isotropic material properties were replaced by orthotropic material properties. The second approach uses the energy method along with an orthotropic constitutive system developed by Pandey at. al (1995). This approach failed to account for the importance of load height above the shear center and bending-twisting coupling effects. The third approach was derived to account for these deficiencies in order to predict

more accurately the lateral-torsional buckling loads for FRP beams. The results using the third formulation are considered in this study. The approximate solution for the critical lateral-torsional buckling load is derived to be as follows (Stoddard, 1997):

$$P_{cr} = \frac{17.199}{L^2}\sqrt{GJ.I_{yy}}\left[\sqrt{1+\frac{\pi^2 I_{\omega\omega}}{L^2 GJ}+2.989\frac{\alpha_{sc}^2 I_{yy}}{L^2 GJ}-0.176\frac{H_s^2}{GJ.I_{yy}}}+1.729\frac{\alpha_{sc}}{L}\sqrt{\frac{I_{yy}}{GJ}}\right] \quad (5.15)$$

where,

P_{cr} : critical load.

L: span length.

G: shear modulus of elasticity.

J: torsional constant.

I_{yy} : minor axis bending stiffness, $E_{a,Y}.I_Y$.

I_Y : minor axis second moment of inertia.

$E_{a,Y}$: apparent modulus of elasticity in minor axis.

$I_{\omega\omega}$: wraping stiffness, $E_{a,Y}.C_\omega$.

C_ω : wraping constant.

α_{sc} : distance between shear center and application of load.

H_s : bending-twisting coupling term.

The bending - twisting coupling term of equation 5.15 (H_s) has been ignored since H_s has relatively no effect (<0.1 %) on the lateral–torsional buckling load for the boundary and loading conditions used (Stoddard, 1997). The distance between the shear center of the cross section and the point at which the

load is applied to the beam (α_{sc}) has a dramatic effect on the lateral–torsional buckling capacity of the member (Stoddard, 1997). The modulus of elasticity in minor axis ($E_{a,Y}$) and the shear modulus of elasticity (G) are considered to be the random variables. Data values (eight specimens) for both variables developed by Stoddared (1997) were used to determine the correlation between them. The correlation coefficient between $E_{a,Y}$ and G was calculated to be -0.660. The correlation coefficient (-0.660) was compared to the value from equation 3.16 (Sachs, 1983) for two sided test at 5% level with degrees of freedom equal to the number of data point minus two (DF=n-2). For n=8, the corresponding value is 0.707. Since the correlation coefficient (0.660) did not exceed the corresponding value using equation 3.16, both $E_{a,Y}$ and G are considered to be independent random variables. Both random variables are assumed to fit the two-parameter Weibull Distribution.

Experimental results for lateral-torsional buckling tests were compared to the analytical results. The ratio of the experimental critical load, $P_{\exp}$, to the analytical critical load, P_{anal}, ranged from 0.8 to 1.24 with an average of 1.07 and a standard deviation of 0.12 (Stoddard, 1997). The ratio of the experimental resistance to the calculated resistance, or the model error, was fit by a normal distribution. The resistance factors were developed using equation 5.15 for all cases of L_n/D_n (0.5, 1.0, 2.0, 3.0, and 4.0). The resistance factor is almost constant with varying L_n/D_n. The average values of the resistance factors are considered in this analysis. All values for the resistance factors are tabulated in

table 14. Based on data developed by Stoddard (1997), $\mu_{E_{a,Y}} / \mu_G$ is assumed to be 9. Changing the ratio $\mu_{E_{a,Y}} / \mu_G$ from 9 to 8 or 10 has relatively no effect (<0.5%) on the resistance factors. Figure 11 shows the resistance factors obtained from equation 5.15 for resistance vs. COV for $E_{a,Y}$ (for all cases of COV of G). Figure 12 shows the resistance factors obtained from equation 5.15 for resistance vs. COV for G (for all cases of COV of $E_{a,Y}$). Figure 11 shows that the resistance factor is almost constant with varying the coefficient of variation of $E_{a,Y}$ for $(CV)_{E_{a,Y}} \leq 0.10$, and decreases with increasing the coefficient of variation of $E_{a,Y}$ for $(CV)_{E_{a,Y}} \geq 0.10$. Figure 12 shows that the resistance factor is almost constant with varying the coefficient of variation of G for all values of COV of $E_{a,Y}$.

A reasonable fit to the data is a constant resistance factor for $(CV)_{E_{a,Y}} \leq 0.10$, and a resistance factor that is a linear function of the coefficient of variation of $E_{a,Y}$ for $(CV)_{E_{a,Y}} \geq 0.10$. The resistance factor using best-fit lines for the data would be:

$$\phi = 1.03 - 0.99\left((CV)_{\mathrm{Ea,\,Y}}\right) \leq 0.93 \qquad (5.16)$$

Thus, it is proposed that rather than a constant resistance factor, the resistance factor be a function of $(CV)_{\mathrm{Ea,\,Y}}$, or the uncertainty level in the FRP material property. The resistance factor would increase with a decreasing coefficient of variation of the modulus of elasticity in minor axis, $E_{a,Y}$, and remain constant with varying the shear modulus of elasticity, G.

Table 14. Resistance Factors for Simply Supported Beams with Lateral-Torsional Buckling Using Equation 5.15.

Resistance Factor (ϕ), L_n/D_n = 0.5							Resistance Factor (ϕ), L_n/D_n = 1						
	COV_E							COV_E					
COV_G	0.05	0.075	0.1	0.15	0.2	0.25	COV_G	0.05	0.075	0.1	0.15	0.2	0.25
0.050	0.920	0.939	0.937	0.887	0.814	0.741	**0.050**	0.906	0.928	0.940	0.913	0.845	0.773
0.075	0.928	0.947	0.946	0.895	0.823	0.749	**0.075**	0.914	0.939	0.951	0.922	0.854	0.782
0.100	0.935	0.954	0.954	0.904	0.831	0.758	**0.100**	0.921	0.947	0.959	0.927	0.862	0.790
0.150	0.949	0.970	0.968	0.918	0.846	0.771	**0.150**	0.937	0.964	0.974	0.946	0.881	0.808
0.200	0.963	0.982	0.981	0.932	0.859	0.787	**0.200**	0.949	0.976	0.987	0.958	0.893	0.823
0.250	0.976	0.995	0.993	0.943	0.872	0.808	**0.250**	0.961	0.990	0.998	0.970	0.906	0.835
Resistance Factor (ϕ), L_n/D_n = 2							**Resistance Factor (ϕ), L_n/D_n = 3**						
	COV_E							COV_E					
COV_G	0.05	0.075	0.1	0.15	0.2	0.25	COV_G	0.05	0.075	0.1	0.15	0.2	0.25
0.050	0.874	0.899	0.917	0.910	0.862	0.797	**0.050**	0.856	0.883	0.903	0.904	0.862	0.802
0.075	0.882	0.908	0.927	0.919	0.871	0.806	**0.075**	0.863	0.891	0.914	0.915	0.871	0.811
0.100	0.889	0.916	0.935	0.928	0.880	0.815	**0.100**	0.870	0.899	0.921	0.924	0.880	0.820
0.150	0.905	0.933	0.953	0.947	0.986	0.831	**0.150**	0.884	0.915	0.936	0.939	0.898	0.839
0.200	0.917	0.947	0.965	0.959	0.911	0.846	**0.200**	0.899	0.928	0.952	0.953	0.911	0.850
0.250	0.930	0.958	0.978	0.971	0.923	0.860	**0.250**	0.912	0.941	0.964	0.966	0.924	0.867
Resistance Factor (ϕ), L_n/D_n = 4							**10**						
	COV_E							COV_E					
COV_G	0.05	0.075	0.1	0.15	0.2	0.25	COV_G	0.05	0.075	0.1	0.15	0.2	0.25
0.050	0.846	0.873	0.894	0.899	0.861	0.805	**0.050**	0.880	0.904	0.918	0.903	0.849	0.784
0.075	0.853	0.881	0.902	0.908	0.870	0.817	**0.075**	0.888	0.913	0.928	0.912	0.858	0.793
0.100	0.861	0.889	0.910	0.971	0.879	0.826	**0.100**	0.895	0.921	0.936	0.931	0.866	0.802
0.150	0.875	0.904	0.927	0.935	0.898	0.842	**0.150**	0.91	0.937	0.952	0.937	0.893	0.818
0.200	0.888	0.918	0.942	0.951	0.915	0.857	**0.200**	0.923	0.950	0.965	0.951	0.898	0.833
0.250	0.903	0.931	0.953	0.963	0.926	0.871	**0.250**	0.936	0.963	0.977	0.963	0.910	0.833

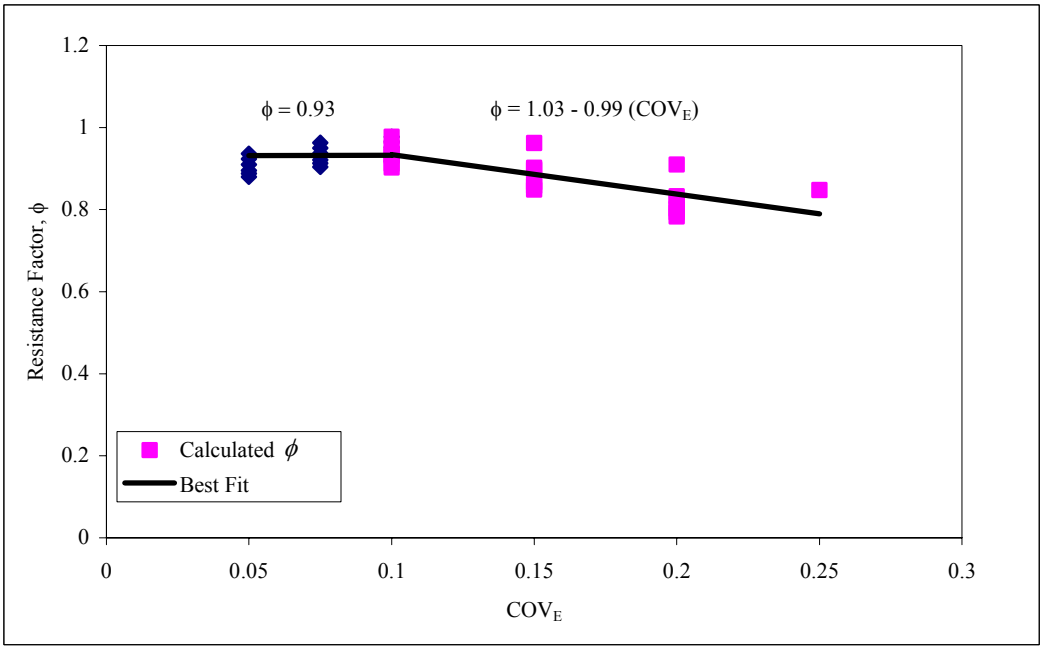

Figure 11. Resistance Factors for Doubly Symmetric Cross Section Beams with Lateral-Torsional Buckling vs. COV of $E_{a,Y}$ for all Cases of COV of G.

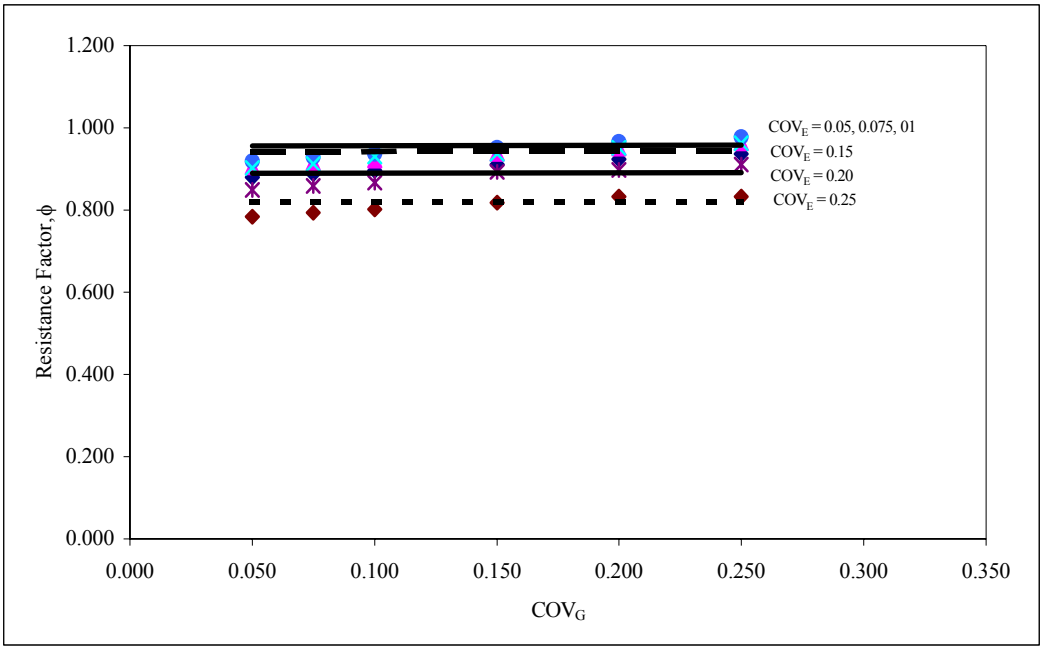

Figure 12. Resistance Factors for Doubly Symmetric Cross Section Beams with Lateral-Torsional Buckling vs. COV of G for all Cases of COV of $E_{a,Y}$.

CHAPTER 6

CONCLUSIONS

Short-term concentrically loaded compression members and simply supported beams loaded with concentrated loads at mid-spans of fiber-reinforced polymeric (FRP) pultruded composite members were investigated using an analytical probabilistic based design procedure. Resistance factors for use in an LRFD format are developed for columns with flexural buckling and local buckling of doubly symmetric sections, both for flexural buckling and flexural-torsional buckling of equal leg angles, and material failure. Resistance factors are developed for lateral-torsional buckling of doubly symmetric simply supported beams with concentrated loads at mid-spans. The resistance factors are based on a target reliability index of 3.0 for buckling failures and 3.5 for material failures. To account for different variabilities in the material properties from different compositions and manufacturing quality control, the developed resistance factors are a function of the coefficient of variation of the appropriate material properties. Creep and long term behavior were outside the scope of the present work and are not considered in this study. It is recommended that creep and long-term behavior be investigated in future work.

Based on the results of the present thesis, model code language can be developed. The factored axial compression resistance load, P_r, for concentrically loaded compression FRP members is found as:

$$P_r = \phi P_n \tag{6.1}$$

where P_n is the nominal resistance and ϕ is the resistance factor. The value of P_r shall not be taken as greater than:

$$P_n = (F_C)_L A_g$$
$$\phi = 1.03 - 2.40\left(CV_{(F_C)_L}\right) \leq 0.79 \tag{6.2}$$

For doubly-symmetric cross-sections, the factored resistance shall not be taken as greater than:

$$P_n = \frac{P_E}{1 + (n_S \ P_E / \ A_g \ G_{LT})}$$
$$\phi = 1.00 - 1.75\left(CV_{E_L}\right) \leq 0.83 \tag{6.3}$$

where P_E is determined as:

$$P_E = \frac{\pi^2 E_L}{\left(\frac{KL}{r}\right)^2_{\min}} A_g \tag{6.4}$$

For cases where E_L/G_{LT} is not greater than 6.0, it is permissible to take P_n as P_E.

For equal-leg angle sections, the factored resistance shall not be taken as greater than either of the following:

$$P_n = \frac{\pi^2 E_L}{\left(\frac{KL_z}{r_z}\right)^2} A_g$$
$$\phi = 0.84 - 1.35\left(CV_{E_L}\right) \leq 0.71 \tag{6.5}$$

$$P_n = 1.2 \frac{G_{LT}}{\left(\frac{b}{t}\right)^2} A_g$$
$$\phi = 0.93 - 0.87\left(CV_{G_{LT}}\right) \leq 0.84 \tag{6.6}$$

For simply supported beams, the factored resistance load, P_r, for mid-span concentrically loaded FRP members is found as:

$$P_r = \phi P_n \tag{6.7}$$

For beams of doubly symmetric sections with concentrated loads at mid-spans, the factored resistance shall not be taken as greater than:

$$P_n = \frac{17.199}{L^2}\sqrt{GJ.I_{yy}}\left[\sqrt{1+\frac{\pi^2 I_{\omega\omega}}{L^2 GJ}+2.989\frac{\alpha_{sc}^2 I_{yy}}{L^2 GJ}-0.176\frac{H_s^2}{GJ.I_{yy}}}+1.729\frac{\alpha_{sc}}{L}\sqrt{\frac{I_{yy}}{GJ}}\right]$$

$$\phi = 1.03 - 0.99\left(CV_E\right) \leq 0.93 \tag{6.8}$$

In all cases, the nominal material properties are the 5-percentile values determined using a Weibull distribution for the data.

REFERENCES

1. – (1993). Load and Resistance Factor Design Specification for Structural Steel Buildings. American Institute of Steel Construction, Chicago, IL.

2. – (1995). Standard for Load and Resistance Factor Design (LRFD) for Engineered Wood Construction. AF&PA/ASCE 16-95, American Forest & Paper Association and American Society of Civil Engineers. New York, NY.

3. – (2002). Minimum Design Loads for Buildings and Other Structures, ASCE 7.

4. Abdallah MH, Abdin EM, Selmy AI, and Khashaba UA. (1996). "Reliability analysis of GFRP pultruded composite rods." International Journal of Quality and Reliability Management, Vol. 13(2), 88-98.

5. Alqam, M., Bennett, R. M., and Zureick, A-H. (2002). "Three-parameter vs. two-parameter Weibull distribution for pultruded composite material properties." Composite Structures, Vol. 58, 497-503.

6. Ang, A. H-S. and Tang, W (1984). Probability Concepts in Engineering Planning and Design, Vol. II, John Wiley & Sons, New York, NY.

7. Barebero, E. and Tomblin, J. (1993). "Euler Buckling of Thin-Walled

Composite Columns," J. of Thin-Walled Structures, Vol.17, 237-258.

8. Brooks, R. J. Turvey, G. J. (1995b). " Lateral Buckling of Pultruded GRP I-Section Cantilevers", Composites Structures, Vol. 32, 203-215.

9. Chambers, R. E. (1997). "ASCE Design Standard for Pultruded Fiber-Reinforced-Plastic (FRP) Structures," Journal of Composites for Construction, 1(1), 26-38.

10. Davalos, J. F., Qiao, P. and Salim, H. A. (1997). "Flexural-torsional buckling of pultruded fiber reinforced plastic composite I-beams: experimental and analytical evaluation." Composite Structures, Vol. 38 No. 1-4, 241-250.

11. Ditlevsen O. (1981). Uncertainty Modeling with Applications to Multidimensional Civil Engineering Systems. New York, NY: McGraw-Hill.

12. Dodson B. (1994). Weibull Analysis. Milwaukee, Wisconsin: ASQ Quality Press.

13. Ellingwood, B.R., Galambos, T.B., MacGregor, J.G., and Cornell, C.A. (1980). Development of a Probability Based Load Criterion for American

National Standard A58. NBS Special Publication 577, U.S. Department of Commerce.

14. Ellingwood, B.R. (1997). "Probability-based LRFD for engineered wood construction." Structural Safety, 19(2), 53-65.

15. Ellingwood, B.R. (2000). Load and Resistance Factor Design (LRFD) for Structures using Fiber-Reinforced Polymer (FRP) Composites. NIST GCR 00-793, National Institute of Standards and Technology.

16. Engesser, F. (1989). "Die Knickfestigkeit Gerader Stabe." *Zeitschrift fur Architekter und Ingeneur Vereins zu Hannover, Weisbaden, Germany, 35, 455 (in German).*

17. Galambos, T.V., Ellingwood, B., MacGregor, J.G., and Cornell, C.A. (1982). "Probability based load criteria: assessment of current design practice", Journal of the Structural Division, ASCE, 108(ST5), 959-977.

18. Gromala, D.S., Sharp, D.J., Pollock, D.G., and Goodman, J.R. (1990). "Load and resistance factor design for wood: the new U.S. wood design specification." International Timber Engineering Conference, Tokyo, Japan, 311-318.

19. Hsiao, L-E, Yu, W-W, and Galambos, T.V. (1990). “AISI LRFD method for cold-formed steel structural members.” Journal of Structural Engineering, ASCE, 116(2), 500-517.

20. Israel, M., Ellingwood, B., and Corotis, R. (1987). “Reliability-based code formulations for reinforced concrete buildings.” Journal of Structural Engineering, ASCE, 113(10), 2235-2252.

21. Kang, J. (2000). “Behavior and Design of Pultruded Fiber Reinforced Polymeric Beams and Beam-Columns Under Sustained Loads.” Master of Science thesis, Georgia Institute of Technology.

22. King, R.L. (1986). “Statistical methods for determining design allowable properties for advanced composite materials.” 15th Reinforced Plastics Conference, British Plastics Federation, Nottingham, England, 79-85.

23. Lawless JF. (1982). Statistical models and methods for lifetime data. New York, NY: John Wiley and Sons.

24. Lee, D. J. and Hewson, P. J. (1978). "The use of fiber-reinforced plastics in thin-walled structures." Stability problems in engineering structures and components, T. H. Richards and P. Stanely, eds., Elsevier Applied Science, New York, N. Y., 23-55.

25. McNutt, J.A. (1998). “Reliability analysis of FRP composite columns”, Master of Science thesis, The University of Tennessee.

26. MIL-HDBK-17 (1990). The Composites Materials Handbook – MIL 17, Vol. 1 – Guide-lines for Characterization of Structural Materials, Technomic Publishing Co., Lancaster, PA.

27. Mottram JT. (1994). Compression strength of pultruded sheet material. Journal of Materials in Civil Engineering, Vol. 6(2), 185-200.

28. Nethercot, D. A. (1973). " The Effective Length of Cantilevers as Governed by Lateral Buckling", The Structural Engineer, Vol. 51, 161 – 168.

29. Nowak AS. (1995). Calibration of LRFD bridge code. Journal of Structural Engineering, ASCE, Vol. 121(8), 1245-1251.

30. Pandey, M. D., Kabir, M. Z. and Sherbourne, A. N. (1995). “ Flexural-Torsional Stability of Thin-Walled Composite I-Section Beams,” Composites Engineering, Vol. 5, No. 3, 321-342.

31. Rust, S.W., Todt, F.R., Harris, B., Neal, D., and Vangel, M. (1989). “Statistical methods for calculating material allowables for MIL-HDBK-

17." Test Methods for Design Allowables for Fibrous Composites, ASTM STP 1003, 136-149.

32. Sachs, L. (1984). Translation of "Angewandte Statistik," Mathematical Statistics, Springer-Verlag New York Inc.

33. Southwell, R. V. (1932). "On the analysis of experimental observations in problems of elastic stability." Proceedings of the Royal Society, London (A), Vol. 135, 601-16.

34. Stoddard, W. P. (1997). "Lateral-Torsional Buckling Behavior of Polymer Composit I-Shaped Members," Ph.D. Dissertation, Georgia Institute of Technology.

35. Tenn LF. (1981). Statistical analysis of fibrous composite strength data. Test Methods and Design Allowables for Fibrous Composites, ASTM STP 734, 229-244.

36. Timoshenko, S. P. and Gere, J. M. (1961). Theory of Elastic Stability, McGraw-Hill, New York.

37. Tomblin, J. and Barebero, E. (1994). "Local Buckling Experiments on FRP Columns," J. of Thin-Walled Structures, Vol.18, 97-106.

38. Turvey, G. J. (1995a). " Lateral buckling Tests on Rectangular Cross-Section Pultruded GRP Cantilever Beams", Composites: Part B, Vol. 27B, 35-42.

39. Turvey, G. J. (1996a). "Effects of Load Position on the Lateral Buckling Response of Pultruded GRP Cantilevers-Comparisons Theory and Experiment", Composite Structures, Vol. 35, 33-47.

40. Wang, Y. and Zureick, A. (1994). “Characterization of the Longitudinal Tensile Behavior of Pultruded I-Shape Structural Members Using Coupon Specimens,” Composite Structures 29, 463-472.

41. Weibull W. (1951). A statistical distribution function with wide applicability. Applied Mechanics, Vol. 18, 293-297.

42. Yoon, S. J. (1993). “Local Buckling of Pultruded I-Shape Columns”, Ph.D. Dissertation, Georgia Institute of Technology.

43. Zanakis SH. (1979). A simulation study of some simple estimators for the three-parameter Weibull distribution. Journal of Statistical Computing and Simulation, Vol. 9, 101-116.

44. Zureick A, Kang J, and Butz T. (2001). Eccentrically Loaded Pultruded

Members in Compression. Research Report SEMM 01-3, Georgia Institute of Technology, Atlanta.

45. Zureick, A. and Scott, D. (1997). "Short-term behavior and design of Fiber-Reinforced Polymeric Slender Members Under Axial Compression," J. of Composites for Construction, Vol.1, No.4, 140-149.

46. Zureick, A., and Steffen, R. (2000). "Behavior and design of concentrically loaded pultruded angle struts," Journal of Structural Engineering, 126(3), 406-416.

VITA

Maha Khader Alqam was born in Jordan, where she was raised and graduated from High school. She went to the University of Science and Technology in Jordan and received a B.S. in civil engineering in 1993. In 1995, Maha attended graduate school at the University of Tennessee, Knoxville and received a M.S. in 1997 and a Ph.D. in 2003, both in civil engineering.